

**EDITOR**

*Doç. Dr. Murat ÇİFLİKLİ*

**EARTH  
SCIENCE  
ENGINEERING**

*Researches and Evaluations in the Field of*

**March  
2025**

**İmtiyaz Sahibi • Yaşar Hız**  
**Genel Yayın Yönetmeni • Eda Altunel**  
**Yayına Hazırlayan • Gece Kitaplığı**  
**Editör • Doç. Dr. Murat ÇİFTLİKLİ**

**Birinci Basım • Mart 2025 / ANKARA**

**ISBN • 978-625-388-275-4**

© copyright

Bu kitabın yayın hakkı Gece Kitaplığı'na aittir.  
Kaynak gösterilmeden alıntı yapılamaz, izin almadan  
hiçbir yolla çoğaltılamaz.

**Gece Kitaplığı**

**Adres:** Kızılay Mah. Fevzi Çakmak 1. Sokak Ümit Apt  
**No:** 22/A Çankaya/ANKARA Tel: 0312 384 80 40

[www.gecekitapligi.com](http://www.gecekitapligi.com)  
[gecekitapligi@gmail.com](mailto:gecekitapligi@gmail.com)

**Baskı & Cilt**  
Bizim Buro  
**Sertifika No:** 42488

# **Research And Evaluations In The Field Of Earth Science Engineering**

**March 2025**

Editor:  
Doç. Dr. Murat ÇİFTLİKLİ



# İÇİNDEKİLER

## BÖLÜM 1

### CURRENT SEISMICITY OF ÇANAKKALE AND ITS SURROUNDINGS

*Fahriye AKAR*.....1

## BÖLÜM 2

### CLASSIFICATION OF METAMORPHIC ZONES AND FACIES

*Gizem ARSLAN* .....19

## BÖLÜM 3

### INVESTIGATION OF TRAVERTINE CAVE STALAGMITES IN TAZEKENT VILLAGE (DIYADIN, AĞRI); ORIGIN AND CLIMATE INTERPRETATIONS

*Çetin YEŞİLOVA, Erhan GÜLERYÜZ,  
Pelin GÜNGÖR YEŞİLOVA, R. Burak TAYMUŞ*..... 29

## BÖLÜM 4

### EFFECT OF FACIES PROPERTIES ON PHYSICOMECHANICAL PROPERTIES: HEYBELİ TRAVERTINES (ADILCEVAZ, BITLİS)

*Çetin YEŞİLOVA, Halit UVAÇIN, Hakan ELÇİ*.....51



# CHAPTER 1

## CURRENT SEISMICITY OF ÇANAKKALE AND ITS SURROUNDINGS

*Fahriye AKAR*<sup>1</sup>

---

1 Assistant Professor Fahriye AKAR, Erzincan Binali Yıldırım University  
Earthquake Technologies Institute and Vocational School,  
Construction Department  
fahriyeakar@erzincan.edu.tr  
ORCID No: 0000-0002-8445-0353

## 1. Introduction

Turkey is located in an important earthquake zone due to its active fault lines and tectonic structure and has been subject to devastating earthquakes throughout history. For this reason, seismic hazard assessments in different regions of the country are of great importance. The Gutenberg-Richter relation, one of the most frequently used methods in the scientific assessment of earthquake hazard, is a basic approach for analyzing the magnitude-frequency relationship of earthquakes in a region (Gutenberg and Richter, 1944). The  $b$  value in this relation is a critical parameter that defines the ratio of small and large earthquakes in a region and is of great importance in seismotectonic analyses and earthquake risk assessments. A high  $b$  value indicates that small earthquakes are more frequent, while a low  $b$  value indicates that the probability of larger earthquakes increases. In studies conducted on the “ $b$ ” value in the earthquake magnitude distribution, it has been determined that the  $b$  value has different average values for different regions. For example, there is a large literature emphasizing that it is 0.84 for Swedish earthquakes, 0.95 for California earthquakes, and higher than 1.5 in one region in China (Turcotte, 1986, Shi and Bolt, 1982, Wang, 1994, Pacheco et al., 1992). Studies conducted throughout Turkey have also revealed that  $b$  value distributions in different tectonic regions of the country show significant differences. In a study conducted by Kalyoncuoğlu et al. (2007),  $B$  values were examined by dividing various regions of Turkey into sub-regions and significant regional differences were detected. For example, in various studies on the North Anatolian Fault, it has been found that the  $b$  value varies according to segments and that regional tectonic movements affect faulting processes (Raub, C. et al. (2017), Öztürk and Bayrak, 2012). In the study by Bohnhoff, M. et al. (2016), which investigated the maximum earthquake magnitudes and  $b$ -value changes in different sections along the North Anatolian Fault Zone, it was explained how different stress conditions and crustal heterogeneities affect the  $b$ -value. Studies conducted on the fault segments in the Marmara Sea and its surroundings have shown that this region carries an active seismic hazard and the  $b$  value is lower, especially in the western parts (Kalafat et al., 2011). In addition, studies conducted in Western Anatolia, such as İzmir and its surroundings, have pointed out high  $b$  value distributions due to the stress regime in the region (Aydan and Hasgür, 2020). Studies conducted in Western Anatolia, especially in regions under extensional tectonics, show that earthquakes in this region are mostly small and medium-sized and therefore the  $b$  value is high. Bayrak et al. (2017) analyzed earthquakes in Western Anatolia between 1900-2010 and determined that the  $b$  value in the region is generally high. Tüfekçi et al. (2010) investigated the relationship between geothermal potential and  $b$  value in Western Anatolia and

examined the effects of earthquakes on geothermal energy resources. In studies conducted in Eastern Anatolia and Southeastern Anatolia regions, different seismic characteristics were observed. B values were generally found to be high along the Eastern Anatolian Fault Line, which increases the frequency of small and medium-sized earthquakes and shows that large earthquakes occur rarely (Karakus et al., 2015). Öztürk and Bayrak (2012) suggested that the b value also varies between segments on the Eastern Anatolian Fault Line and that these differences are related to regional tectonic stresses. In addition, Akar (2024) evaluated the effects of earthquakes and changes over time by examining the b value changes associated with the 2023 Kahramanmaraş earthquakes. It was determined that the b value was low due to the stress increase before the major earthquakes. Çubuk et al. (2018) analyzed the b value distributions in Erzincan and its surroundings, contributing to the assessment of the seismic risk of the region. Çanakkale and its surroundings are under significant seismic hazard due to their location at the western end of the North Anatolian Fault. Earthquakes that occurred especially in the Ganos Fault and Saros Bay indicate that seismic activity in the region is high. In this study, the b value distribution was analyzed via the Gutenberg-Richter relation using earthquakes that occurred in Çanakkale and its surroundings. The b value plays a key role in understanding the tectonic stress accumulation and potential earthquake hazard of the region. These analyses will provide significant contributions to better understand the seismic behavior of the region and develop strategic plans for earthquake risk management.

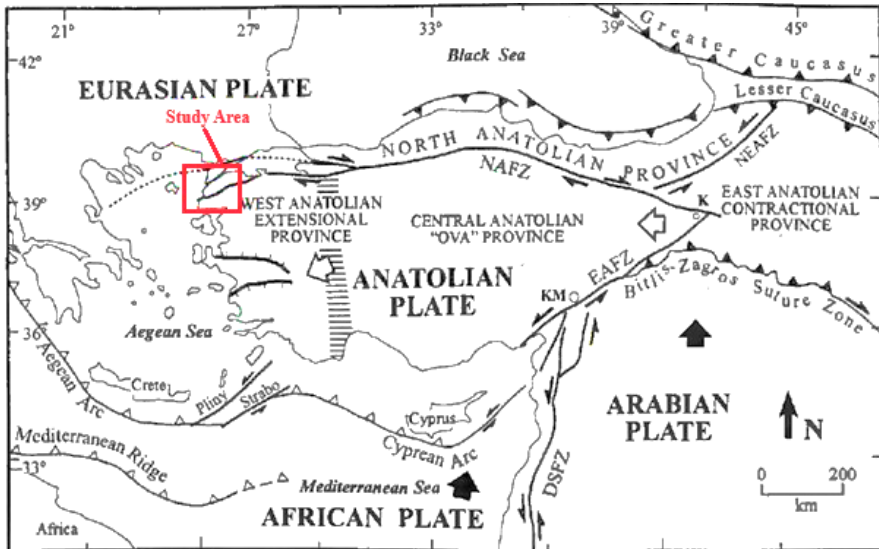


**Figure 1.** Simplified tectonic map of Turkey showing the main neotectonic structures and neotectonic regions (Bozkurt, 2001). Thick lines indicate strike-slip faults, solid triangles indicate fold and thrust belts, open triangles indicate

*active subduction zones, and hatched lines indicate normal faults. Thick arrows indicate the relative direction of motion of the African and Arabian plates, and open arrows indicate the motion of the Anatolian Plate. The hatched area indicates the transition zone between the Western Anatolian extensional zone and the Central Anatolian “plain” region.*

## 2. Regional Tectonic Structure

Turkey has been showing a distinct seismotectonic activity since the neotectonic period, as the intersection point of the Arabian, Eurasian and African plates (Şengör et al. 2005; Reilinger et al. 2006). These processes provide the westward movement of the Anatolian Plate relative to the Eurasian Plate (Le Pichon et al., 1995; Reilinger et al., 2006) and this movement is controlled by the North Anatolian Fault Zone (NAFZ). The westward movement of the Anatolian Block has been measured as 25–30 mm per year by GPS data (McClusky et al., 2000). The NAFZ is an active transform fault extending approximately 1600 km from Eastern Anatolia to the Aegean Sea, and this fault contains compressional tectonic features resulting from the collision of the Arabian and Anatolian plates in eastern Turkey, while in the west, it triggers extensional deformations due to the subduction effect of the African plate. After entering the Marmara Region in the west, the NAFZ splits into three main branches (Barka and Kadinsky-Cade, 1988; Emre et al. 2012). The northern branch passes under the Marmara Sea and reaches the Gulf of Saros; the middle branch follows the Osmaneli-Gemlik-Bandırma line; and the southern branch follows the Geyve-Yenişehir-Bursa-Gönen-Edremit line (Barka, 1992; Taymaz et al. 1991; Nyst and Thatcher 2004; Müller et al. 2012; Kürçer et al. 2016). This deformation zone covers a wide area starting from Thrace to the Aegean graben system (Kreemer et al., 2004). Therefore, Çanakkale and the Biga Peninsula are one of the most active seismotectonic regions of northwestern Anatolia. In this region, in addition to the NAFZ, other major seismotectonic structures include the Yenice-Gönen Fault (YGF), Biga-Çan Fault (BÇF) and Ganos Fault (GF) (Barka et al., 1997; Kürçer et al., 2009). These fault branches, starting from the Marmara Region and extending to the Aegean Sea, have produced major earthquakes both in the historical and instrumental periods, and the seismic potential of these faults is quite high (Ambraseys, 2001; Nalbant et al., 1998). Of these faults, the Yenice-Gönen and Ganos faults in particular have produced major earthquakes throughout history. In particular, the earthquake with a magnitude of  $M_s=6.8$  that occurred off the coast of Ayvacık–Edremit on October 6, 1944, the earthquake with a magnitude of  $M_s=7.2$  that occurred in Yenice on March 18, 1953, the earthquake with a magnitude of  $M_s=7.0$  that occurred in Manyas, Balıkesir on October 6, 1964, and the earthquake with a magnitude of  $M_w=6.1$  that occurred in Biga on July 5, 1983 were

associated with these faults and revealed the seismic potential of the region (McKenzie, 1972; Taymaz et al., 1991). The region is also under the influence of the extensional regime in the Aegean Sea (Koukouvelas and Aydin, 2002). This extensional regime affects local faulting systems and triggers both strike-slip large faults and normal faulting (Jolivet et al., 2012). In the Biga Peninsula, northeast-oriented strike-slip movement is dominant, and a transition to normal faulting is observed in the south of the peninsula (Kiratzi, 2002). The southern part of the Biga Peninsula has attracted attention with increased seismic activity in recent years. In particular, the 2017 earthquake swarm in the Ayvacık region revealed how tectonically active the region is (Kalafat et al., 2009). Earthquakes in the region generally occur at depths of less than 25 km, close to the surface, reflecting the shallow structure of the faults and the active tectonic character of the region (Erdik et al., 2004; Bohnhoff et al., 2016). In conclusion, the Biga Peninsula and the Çanakkale area are a region with high seismic activity, both under the influence of the North Anatolian Fault Zone and as part of the extensional tectonics in the Aegean region. These active fault systems control the seismicity of the region and have produced major earthquakes throughout history (Kalafat et al., 2009). The Biga Peninsula and its surroundings are among the regions of Turkey with significant earthquake risk due to their complex tectonic structure, high seismic activity and a history full of historical earthquakes. Therefore, it is of great importance to understand seismic activities and their regional effects, to estimate future seismic hazards and to collect the necessary information to reduce these risks.

### 3. Data and Method

The Gutenberg-Richter relationship defines a mathematical relationship between the frequency and magnitude of earthquakes and has an important place in the field of seismology. Developed by Charles F. Richter and Beno Gutenberg, this relationship describes the magnitude distribution of earthquakes occurring in a region in a certain time period. This relationship is one of the basic models used to estimate the magnitude and frequency of earthquakes.

The Gutenberg-Richter relationship is expressed as the following formula:

$$\log_{10} N(M) = a - bM \quad (1)$$

In this equation,  $N(M)$ : The number of earthquakes with a magnitude of  $M$  or greater.  $a$ : A constant indicating the general seismic activity level of the region.  $b$ : The parameter that determines the magnitude distribution of earthquakes and defines the relationship between frequency and magnitude (Gutenberg & Richter, 1956).

The  $b$  value, which is an important component of this relationship, plays a critical role in defining the magnitude distribution and frequency of earthquakes. Using data obtained from earthquake catalogs, the  $b$  value in a region can be calculated to obtain information about the seismic characteristics of that region (Scholz, 2015). The  $b$  value may vary depending on the tectonic features of the region. Generally, the  $b$  value is found to be around 1 for earthquakes worldwide (Frohlich and Davis, 1993). However, this value may vary significantly from region to region (Wiemer & Wyss, 2000). The tectonic structure in a region greatly affects the  $b$  value. A  $b$  value of less than 1 is observed in regions where large earthquakes occur more frequently than small earthquakes and where there is high stress accumulation. Such regions are usually large fault zones or plate boundaries (Scholz, 2015).  $B$  values greater than 1 are frequently encountered in regions where small earthquakes are more common, where there is low stress accumulation or in volcanic regions (Mogi, 1962). The calculation of the  $b$  value is usually done by two methods: the least squares method and the maximum likelihood method. The least squares method is performed by subjecting logarithmically transformed magnitude and frequency data to linear regression analysis. The maximum likelihood method offers a more statistical approach, minimizing errors that may be caused by missing data (Aki, 1965). The completeness of earthquake catalogs is extremely important for the accuracy of the  $b$  value. The minimum magnitude threshold of an earthquake catalog has a great effect on the  $b$  value. Inadequate catalogs or catalogs that do not record small earthquakes may cause incorrect calculations of the  $b$  value (Wiemer & Wyss, 2000). The  $b$  value may change over time or in different areas. These changes may be due to various geological processes such as tectonic stress accumulation, fault activity or volcanic activity (Gutenberg & Richter, 1944). Seismotectonic zones and geological age, thermal gradient, crack density, fault length, seismic wave speed changes, pore pressure and anisotropy, mechanical properties of materials and stress conditions are the factors affecting the  $b$  value (Mogi, 1967, Miyamura, 1962, Ogata et al., 1991; Schorlemmer et al., 2005; Scholz, 2015, Abdelfattah et al., 2020). The  $b$  value also helps to understand the seismic hazard potential of the region. For example, a low  $b$  value indicates a region where large earthquakes may occur more frequently and therefore the seismic risk is high. When conducting seismic risk analyses in such regions, it is critical to consider the  $b$  value (Wiemer & Wyss, 2000).

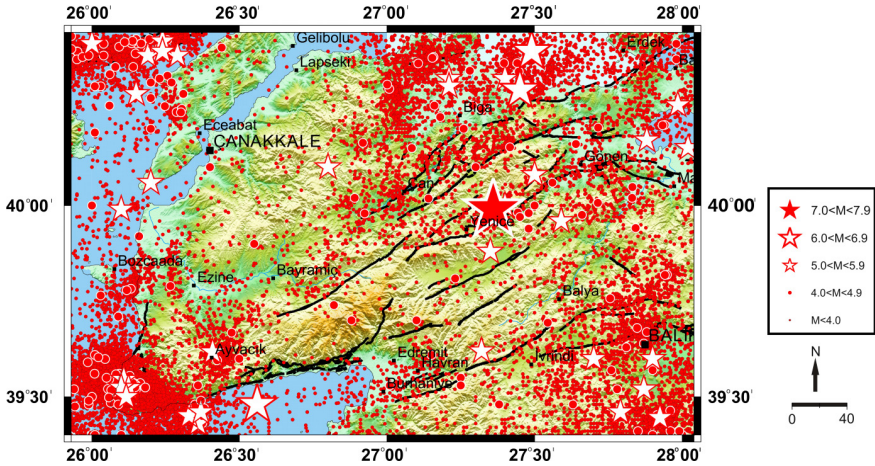
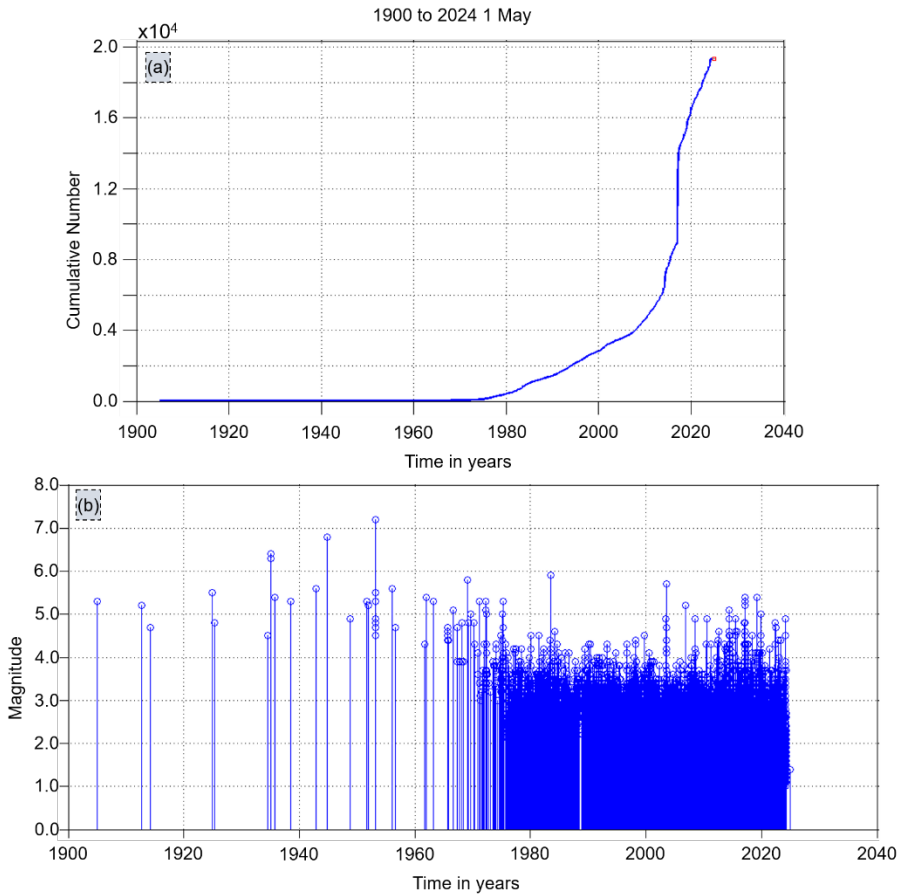


**Figure 2:** Map showing distribution of earthquakes of the study area for the period of 1900-2024.

## Results

The figure 2 shows the 19326 earthquakes that occurred in Çanakkale and its vicinity from 1900 to the present with a magnitude greater than  $M_w 1$ . The largest earthquake ( $M_w=7.2$ ) was the 1953 Yenice earthquake. There were 3 earthquakes with magnitudes between 6 and 7, 33 with magnitudes between 5 and 6, 178 with magnitudes between 4 and 5, 2316 with magnitudes between 3 and 4, 9673 with magnitudes between 2 and 3, and 7122 with magnitudes between 1 and 2. The majority of the earthquakes occurred at depths less than 35 km. While drawing the Gutenberg-Richter relation, the catalogue was de-clustered (Reasenber, 1975) in order to reflect tectonic features. Thus, the new catalogue obtained after declustering, which included 11214 earthquakes, was used in the b-value calculation. With this process, 8610 dependent earthquakes were removed from the catalog. In this study, the maximum likelihood estimation method was used because it provides a more robust estimate than the least squares regression technique (Aki, 1965) in calculating the b value. Especially in seismicity studies, the completeness magnitude ( $M_c$ ) is required in estimating the b value in the Gutenberg-Richter relation.  $M_c$  values for the study area were found to be 2.7 in the selected time interval. The b value was estimated as  $0.94 \pm 0.01$ . It is seen from the graph of the b value depending on time that the values decrease over time. Figure 6 shows the distribution of the b value in 5 km depth intervals up to 25 km. With this process, b value changes at different depths were analyzed. These depths are 0-5, 5-10, 10-15, 15-20, 20-25 depth intervals. And in order to determine the b value change for these depth intervals, earthquakes at these depths were used. The b-value was calculated using the moving window approach in the maximum cur-

vature method (in Woessner and Wiemer, 2005) and was associated with seismicity. A grid interval of  $0.03 \times 0.03$  was selected. When the patterns of the b value obtained from these calculations with depth were examined, it was observed that it generally varied between 0.4 and 2 and that the b value increased with increasing depth. It was observed that the b value was high especially in all depth layers except for 5 km on the Aegean Sea side. On the other hand, it is noteworthy that the Marmara Sea side exhibited low b values at all depths. In addition, b values decreased in the first 10 km around the Biga-Çan Fault Zone and around the fault segments between Edremit-Balıkesir.



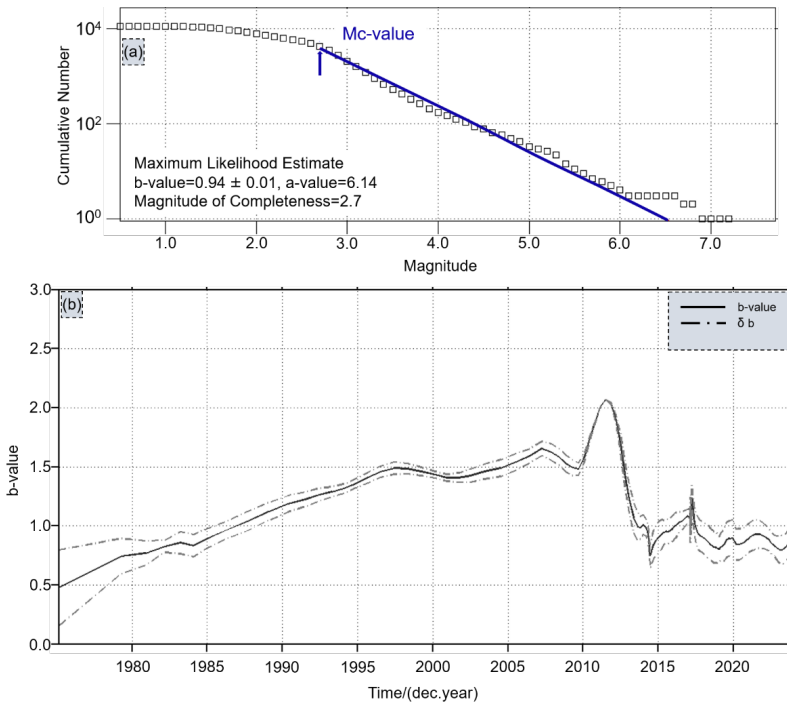
**Figure 3.** **a)** Cumulative number of earthquakes near Çanakkale. **b)** Time-dependent change in the magnitudes of earthquakes from 1900 to 2024.

Figure 3 shows the distribution of earthquakes that occurred in Çanakkale and its surroundings over time between 1900 and 2024.

The upper part of the graph shows the increase in the total number of earthquakes recorded over time. While a relatively low increase was observed in the early 1900s, a significant acceleration is observed after the 1980s. This rapid increase can most likely be attributed to the widespread use of seismic networks, improved recording systems, and the detection of more earthquakes due to technological developments. In the 2020s, a steeper rise is observed in the curve. This situation may be explained by a real increase in the frequency of earthquakes in the region, or by more intensive monitoring of the region.

The lower graph shows the magnitude of each earthquake on the time axis. Many earthquakes of different magnitudes have been recorded since the early 1900s. An intense increase in data after 1980 is striking. This shows that seismic activity in the region is continuously monitored and even small-scale earthquakes are recorded. However, major earthquakes have occurred from time to time and are evident as points seen vertically at higher levels.

In general, these graphs show that seismic activity in Çanakkale and its surroundings has been increasingly monitored towards the end of the 20th century and that there has been a significant increase in the number of recorded earthquakes, especially in recent years. Examining the seismotectonic structure of the region is important in understanding the recurrence periods of major earthquakes and assessing potential future risks.



**Figure 4.** a) Gutenberg-Richter relation of earthquakes from 1900 to 2024. b) Time-dependent  $b$ -value variation obtained from earthquakes.

Figure 4 examines the Gutenberg-Richter relationship and the time-dependent change of the  $b$ -value for earthquakes that occurred between 1900-2024.

The relationship between earthquake magnitudes and their cumulative number is evaluated within the framework of the Gutenberg-Richter law. This law predicts that small earthquakes occur much more frequently than large earthquakes in a given region. The graph in the figure shows this relationship on a logarithmic scale.

The linear trend that best fits the obtained data is defined by the Gutenberg-Richter equation. As a result of the analysis,  $M_c$  (Completeness Value of Magnitude) = 2.7 was determined. This value indicates that smaller earthquakes may have been missing or inadequately recorded. In addition, the calculated  $b$ -value = 0.94, which provides important information about the seismic stress status in the region. The  $b$ -value is expected to be around 1 in typical tectonic regions. A lower  $b$ -value indicates that large earthquakes occur relatively more frequently, while a higher  $b$ -value indicates that small earthquakes predominate.

The Gutenberg-Richter relationship is of great importance in analyzing the statistical distribution of earthquakes in the region. Such analyses play a critical role in earthquake hazard assessments and can provide important information about the probability of large earthquakes occurring in the region.

The change in the b-value over time is considered an important parameter for understanding the evolution of seismic activity in the region. When the graph below is examined, a gradual increase in the b-value is observed since the 1980s. This increase indicates that the number of smaller earthquakes in the region has increased or that the stress release in the fault system has changed.

A sudden increase in the b-value is observed especially between 2010 and 2015. Such sudden changes usually occur before or after a large earthquake. During this period, a significant change may have occurred in the seismotectonic processes in the region.

In recent years, a decrease in the b-value has been observed. This may indicate that the probability of large earthquakes has increased. A decrease in the b-value before major earthquakes usually indicates that stress is accumulating in the fault zone and that the potential for a major rupture is increasing.

In general, the temporal variation of the b-value is a critical parameter for understanding how seismic activity in the region evolves. In particular, sudden changes that occur before or after major earthquakes provide valuable information about the stress accumulation and release in the region. Such analyses are of great importance in determining earthquake hazard and assessing possible risks.

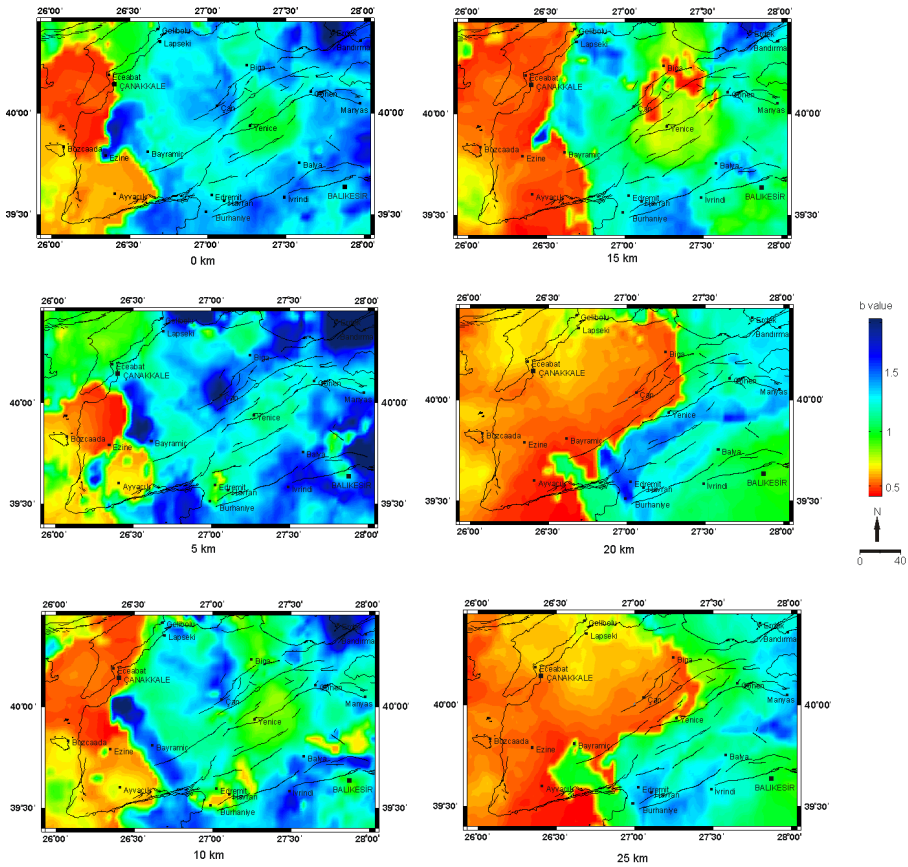


Figure 5. Regional b-value distribution with 0, 5, 10, 15, 20, and 25 km depths.

Figure 5 shows the changes in the regional b-value distribution at different depths. This analysis is of great importance in understanding how seismic activity in the region varies with depth. The b-value is a parameter used in earthquake statistics that determines the ratio of small and large earthquakes in a given region. A high b-value indicates that more small-scale earthquakes occur, while a low b-value indicates that the stress accumulation in the region is high and carries a potential risk for large earthquakes. The spatial distribution of b-values for depths from 0 km to 25 km is mapped in the figure. The color scale shows that blue tones indicate high b-values, while red and yellow tones indicate low b-values. High b-values are observed near the surface, especially in Çanakkale and its surroundings. This shows that the stress release in the region is more regular and that smaller-scale seismic activities are dominant instead of large earthquakes. However, as the depth increases, especially in the eastern and southeastern regions after 15 km, the b-value decreases significantly. The-

se areas, represented by red and orange colors, are considered as regions with high stress accumulation and risk for major earthquakes.

Especially in Ezine, Bayramiç and its surroundings, low b-values are striking at depths of 15 km and deeper. It can be said that there is high stress accumulation in these regions and the probability of major earthquakes increases. In contrast, relatively high b-values are observed in Gelibolu and some other areas in the northwest. This indicates that there is lower stress accumulation in these regions and that major earthquakes are less likely.

In general, this study presents a detailed spatial distribution of seismic hazard in the region. While areas with low b-values pose a potential risk for major earthquakes due to high stress accumulation, it is seen that more small-scale earthquakes occur in areas with high b-values. In addition, a significant decrease in b-values as depth increases indicates that suitable conditions for major earthquakes occur, especially in the lower sections of faults. Such analyses are of great importance in determining the earthquake hazard in the region and in terms of measures to be taken in the future. Future studies may provide more comprehensive information about the probability of major earthquakes by examining the changes in stress accumulation in the region over time.

## Conclusions

In this study, the b-value distribution of the Çanakkale and surrounding region was examined and the spatial and temporal changes of seismic activity were evaluated in detail. The b-value is an important parameter that determines the rate of small and large earthquakes in a region and provides critical information about stress accumulation and release in fault zones. The analyses performed have revealed important results in terms of understanding how the seismic hazard in the region changes at different depths and over time.

First of all, the analyses of the cumulative number and magnitude of earthquakes that occurred from 1900 to the present reveal that seismic activity in the region has increased significantly, especially after the 2000s. With the earthquake records becoming more comprehensive since the 1980s, the detection of small-scale earthquakes has become easier and this has caused a sharp increase in the cumulative number of earthquakes. The increase in small and medium-sized earthquakes in recent years provides important clues about stress accumulation and fault activity in the region.

When the b-value change of Çanakkale and its surroundings is examined over time, it is seen that there are fluctuations in certain periods. While

relative increases in b-values have been observed since the beginning of the 2000s, there have been significant decreases in some critical periods (for example, between 2010-2015). These changes in b-values are directly related to the stress releases in the fault system and the statistical distribution of earthquakes in the region. While low b-values indicate that the stress accumulation in the region has increased and that there may be a potential for a large earthquake, high b-values indicate that smaller-scale earthquakes are dominant and that the stress is released more regularly.

b-value analyses performed depending on the depth have revealed how seismic activity in Çanakkale and its surroundings varies from surface to depth. It is observed that the b-value is generally high at shallow levels between 0-10 km and that small-scale earthquakes are dominant in these regions. However, it has been observed that the b-value decreases significantly as we go down to levels of 15 km and deeper, especially around Ezine, Bayramiç and Çan districts. This situation shows that there is higher stress accumulation in these regions and that they carry a potential risk for large earthquakes. The decrease in b-value, especially after 20 km, suggests that deep fault segments may be at a critical stress threshold.

Considering the tectonic structure of Çanakkale, it is seen that the seismic activity in the region is related to the western extensions of the North Anatolian Fault and the complex fault systems that include Edremit Bay. These faults contain both strike-slip and normal fault components due to the effect of extensional tectonics in the Aegean Sea. Therefore, it is expected that the b-value distribution in the region is heterogeneous. However, the low b-values observed as the depth increases may be an important sign in terms of determining potential areas that can produce large earthquakes.

In conclusion, b-value analyses in Çanakkale and its surroundings have revealed how seismic activity in the region changes depending on time and space. It was understood that the b-value decreases as the depth increases and stress accumulation is higher in certain regions. This situation shows that areas with low b-values in particular should be carefully monitored in terms of large earthquakes. More detailed analyses to be conducted in the future will provide significant contributions to seismic hazard assessments by revealing more clearly the changes in stress accumulation in these regions over time.

## References

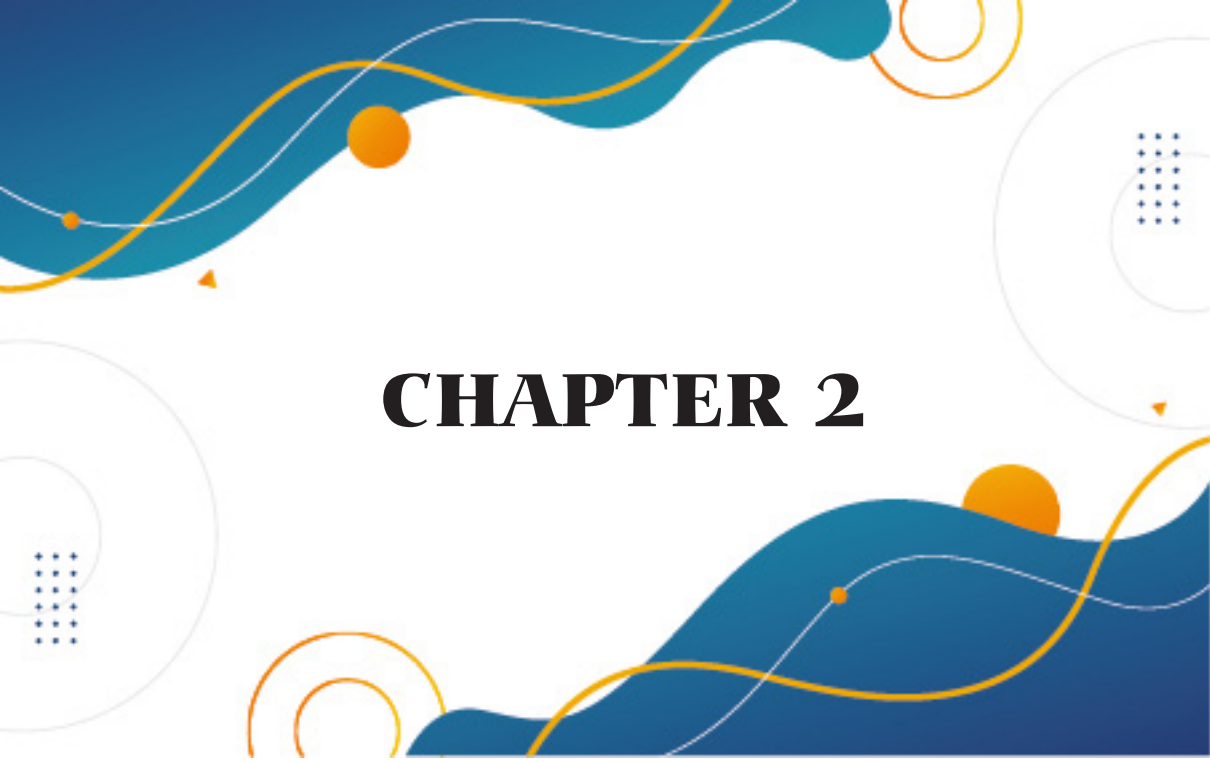
- Ambraseys, N. (2001). The earthquake of 10 July 1894 in the Gulf of Izmit (Turkey) and its relation to the earthquake of 17 August 1999. *Journal of Seismology*, 5(1), 117-128. <https://doi.org/10.1023/A:1011470210656>
- Barka, A. A. (1992). The North Anatolian fault zone. *Annales Tectonicae*, 6(1), 164-195.
- Barka, A. A., & Kadinsky-Cade, K. (1988). Strike-slip fault geometry in Turkey and its influence on earthquake activity. *Tectonics*, 7(3), 663-684. <https://doi.org/10.1029/TC007i003p00663>
- Barka, A. A., Akyüz, H. S., Altunel, E., Sunal, G., Çakır, Z., Dikbaş, A., ... & Armijo, R. (1997). The surface rupture and slip distribution of the 17 August 1999 Izmit earthquake (M 7.4). *Seismological Research Letters*, 70(4), 20-29. <https://doi.org/10.1785/gssrl.70.4.20>
- Bohnhoff, M., Martínez-Garzón, P., Bulut, F., Stierle, E., & Ben-Zion, Y. (2016). Maximum earthquake magnitudes along different sections of the North Anatolian fault zone. *Tectonophysics*, 674, 147-165. <https://doi.org/10.1016/j.tecto.2016.02.028>
- Bozkurt, E. (2001). Neotectonics of Turkey—a synthesis. *Geodinamica Acta*, 14(1-3), 3-30. <https://doi.org/10.1080/09853111.2001.11432432>
- Emre, Ö., Duman, T. Y., Özalp, S., Şaroğlu, F., Olgun, Ş., Elmacı, H., & Çan, T. (2012). Active fault map of Turkey. General Directorate of Mineral Research and Exploration, Special Publication Series 30, Ankara, Turkey.
- Erdik, M., Fahjan, Y., Demircioğlu, M., Sesetyan, K., Durukal, E., & Siyahi, B. (2004). Istanbul Earthquake Rapid Response and the Early Warning System. *Bulletin of Earthquake Engineering*, 2(4), 155-175. <https://doi.org/10.1007/s10518-004-2291-5>
- Jolivet, L., Faccenna, C., Huet, B., Labrousse, L., Le Pourhiet, L., Lacombe, O., ... & Doutsos, T. (2012). Aegean tectonics: Strain localisation, slab tearing and trench retreat. *Tectonophysics*, 597, 1-33. <https://doi.org/10.1016/j.tecto.2012.06.011>
- Kalafat, D., Kekovalı, K., Horasan, G., & Öcal, A. (2009). Sismoloji ve Türkiye'de Depremsellik. *Deprem Araştırma Dairesi Yayınları*, 21.
- Kiratzi, A. A. (2002). Stress tensor inversions along the westernmost North Anatolian fault zone and its continuation into the North Aegean Sea. *Geophysical Journal International*, 151(2), 360-376. <https://doi.org/10.1046/j.1365-246X.2002.01768.x>
- Koukouvelas, I., & Aydın, A. (2002). Fault structure and related basins of the North Anatolian Fault Zone in the Bolu pull-apart region, Turkey. *Journal of Geophysical Research: Solid Earth*, 107(B7), ESE 5-1. <https://doi.org/10.1029/2001JB000398>

- Kreemer, C., Holt, W. E., Goes, S., & Govers, R. (2004). Modeling the neotectonics of the Aegean region. *Geophysical Journal International*, 157(3), 1377-1392. <https://doi.org/10.1111/j.1365-246X.2004.02272.x>
- Kürçer, A., Akyüz, H. S., Altunel, E., Meghraoui, M., Ferry, M., & Dikbaş, A. (2009). Neotectonic structure and earthquake potential of the Yenice-Gönen fault. *Journal of Asian Earth Sciences*, 34(5), 586-596. <https://doi.org/10.1016/j.jseaes.2008.10.003>
- Kürçer, A., Meghraoui, M., Akyüz, H. S., Ferry, M., Dikbaş, A., & Güneç, K. (2016). Yenice-Gönen fault (NW Turkey): Active tectonics and future earthquake potential. *Tectonics*, 35(1), 115-133. <https://doi.org/10.1002/2015TC003890>
- Le Pichon, X., Şengör, A. M. C., Demirbağ, E., Rangin, C., İmren, C., Armijo, R., ... & Görür, N. (1995). The active main Marmara fault. *Earth and Planetary Science Letters*, 129(1-4), 213-231. [https://doi.org/10.1016/0012-821X\(94\)00249-4](https://doi.org/10.1016/0012-821X(94)00249-4)
- McClusky, S., Balassanian, S., Barka, A., Demir, C., Ergintav, S., Georgiev, I., ... & Reilinger, R. E. (2000). GPS constraints on plate kinematics and dynamics in the eastern Mediterranean and Caucasus. *Journal of Geophysical Research: Solid Earth*, 105(B3), 5695-5719. <https://doi.org/10.1029/1999JB900351>
- McKenzie, D. P. (1972). Active tectonics of the Mediterranean region. *Geophysical Journal International*, 30(2), 109-185. <https://doi.org/10.1111/j.1365-246X.1972.tb02351.x>
- Müller, B., Sperner, B., Heidbach, O., Fuchs, K., & Delvaux, D. (2012). World stress map database as a resource for studies of tectonic stress. *Geophysical Journal International*, 140(2), 155-162. <https://doi.org/10.1046/j.1365-246x.2000.00042.x>
- Nalbant, S. S., Hubert, A., & King, G. C. (1998). Stress coupling between earthquakes in northwest Turkey and the North Aegean Sea. *Journal of Geophysical Research: Solid Earth*, 103(B10), 24469-24486. <https://doi.org/10.1029/98JB01491>
- Nyst, M., & Thatcher, W. (2004). New constraints on the active tectonic deformation of the Aegean. *Journal of Geophysical Research: Solid Earth*, 109(B11), 1068-1075. <https://doi.org/10.1029/2003JB002830>
- Reilinger, R., McClusky, S., Vernant, P., Lawrence, S., Ergintav, S., Çakmak, R., ... & Özener, H. (2006). GPS constraints on continental deformation in the Africa-Arabia-Eurasia continental collision zone and implications for the dynamics of plate interactions. *Journal of Geophysical Research: Solid Earth*, 111(B5), 2010-2022. <https://doi.org/10.1029/2005JB004051>
- Şengör, A. M. C., Tüysüz, O., İmren, C., Sakınç, M., Eyidoğan, H., Görür, N., ... & Le Pichon, X. (2005). The North Anatolian Fault: A new look. *Annual Re-*

view of Earth and Planetary Sciences, 33, 37-112. <https://doi.org/10.1146/annurev.earth.32.101802.120523>

Taymaz, T., Jackson, J., & McKenzie, D. (1991). Active tectonics of the North and Central Aegean Sea. *Geophysical Journal International*, 106(2), 433-490. <https://doi.org/10.1111/j.1365-246X.1991.tb03906.x>





# CHAPTER 2

## CLASSIFICATION OF METAMORPHIC ZONES AND FACIES

*Gizem ARSLAN*<sup>1</sup>

---

<sup>1</sup> Research Assistant Dr. Gizem Arslan, Firat University, Faculty of Engineering, Department of Geological Engineering, g.arslan@firat.edu.tr, ORCID No: 0000-0002-8727-7509

## 1. Introduction

Metamorphism is the process of mineralogical, chemical, and physical changes that occur in the depths of the Earth's crust due to the exposure of existing rocks to high temperature and pressure conditions. This process changes the mineral composition and texture of the rocks without melting.

## 2. Zones of Metamorphism

The mineral assemblage found in a metamorphic rock is transformations or newly formed types of minerals of the minerals belonging to the original rock formed by adapting to new physical and chemical conditions under metamorphic conditions.

Since pressure and temperature, the main factors influencing metamorphism, are closely related to depth, it is logical to classify metamorphic zones based on their depth, if the chemical composition is taken into account. In this context, metamorphism zones are divided into three depth zones: *epizon, mesozone and, catazone*.

**Epizone: The upper zone** where the temperature is low to moderate, lithostatic pressure is low and stress is mostly high (though sometimes absent). The most typical minerals of the epizon are Fe and Mn containing garnets, actinolite, glaucophane, epidote/zoisite, chlorite, albite, muscovite, talc and anatase. Hydrous silicates are formed as a result of chemical reactions and dynamic metamorphism in the epizone.

**Mesozone: It is the middle zone** where pressure and temperature are higher than in the epizone and stress is very high (though sometimes absent). The characteristic minerals of the mesozone include hornblende, partly actinolite and anthophyllite, disthene, almandine type garnet, epidote/zoisite, plagioclase rich in anorthite, rarely orthoclase, biotite, muscovite, staurolite, phlogopite, chlorite.

**Catazone: The deepest zone** where pressure and temperature are the highest and stress is lower than in other zones. The typical minerals of the catazone are diopside and omphacite type augit, olivine, hornblende, pyrop-almandine-grossular type garnet, cordierite, plagioclase rich in anorthite, alkali hornblende, alkali augit, biotite, orthoclase, spinel and sillimanite.

Minerals that occur in all three metamorphic zones and do not specifically characterize any zone are called “**cheeky minerals**” and these include quartz, titanite, rutile, biotite, calcite, biotite.

### 3. Facies Concept

The concept of facies was introduced by Eskola (1915), despite undergoing many modifications, it is used in a general sense today. The formation and sequence of certain minerals in a rock as a result of changes related to pressure (bar), temperature (°C) and chemical environmental conditions are referred to as metamorphic facies. Each of the facies includes rocks formed in a specific pressure and temperature range and the minerals present in these rocks reflect those conditions.

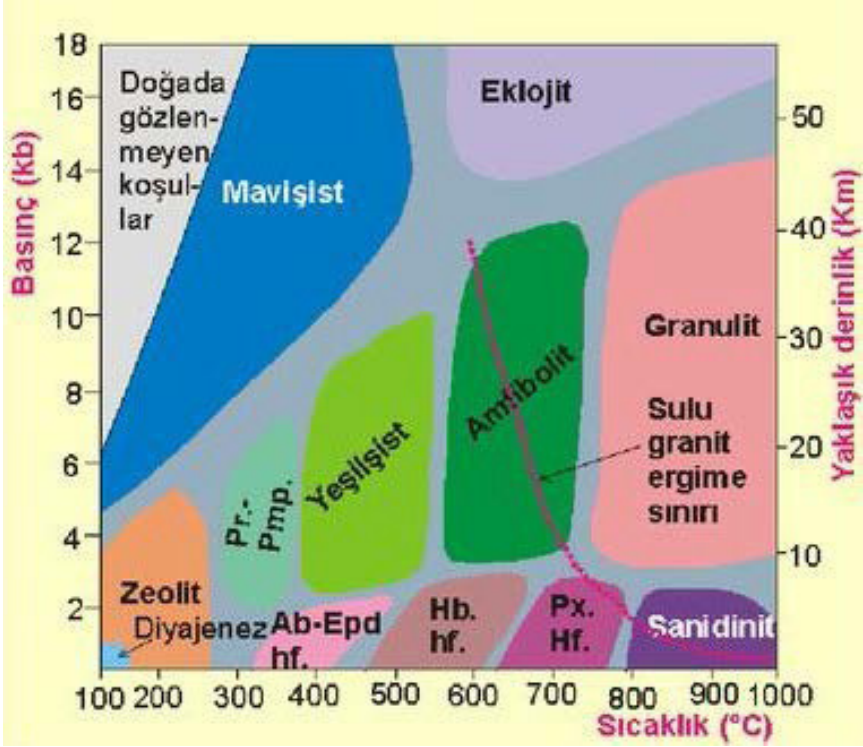


Figure 3.1. Representation of metamorphic facies in temperature and pressure diagram (Yardley, 1989)

#### To summarize;

- The metamorphic facies are not characterized by a single rock type, but are represented by different types of rocks formed under the same conditions along with their corresponding mineral assemblages.
- The boundaries between facies, which are characterized by different mineral assemblages and rock groups formed under diffe-

rent pressure and temperature (P/T) conditions, are not definite but gradually transitional.

- Under the same facies conditions, rocks with the same chemical composition form the same mineral assemblages.

Origin Rocks	Glaucofan-chist Facies ~ 300 °C high pressure	Greenchist Facies 400-550°C low-medium pressure	Amphibolite Facies 550-700°C high pressure	Granulite Facies 700-800°C high to very high pressure	Eclogite Facies > 700°C >8-10 kb
Peridotite and other ultramafites	antigorite-serpentine jadeite	chrysotile-actinolite nephritite talkshist	pyrope-serpentine bronzite-serpentine	pyroxene-granulite enstatite-safirir-granofels	
Mafites Diabase Gabro-basalt Diorite-andesite	Glaucofan schist	metadiabase greenschist epidotit chlorite-albitichist	amphibolite garnet-pyroxene amphibolite hornblend gneiss metaanortoside	granulite pyroxene-granulite hornblend granulite	eclogite hornblende-eclogite
Granitic rocks Granite, granodiorite Tonalite, rhyolite Alkaline granite	metagranite	metagranite protojin gneiss with eyes albit-gnays	granite-gneiss granodiorite-gneiss tonalite-gneiss riebekite-gneiss, alkali-gneiss	granulite scharnochite pyroxene-granulite beachiogranulite	
Arkose Graywacke Conglomerate	Glaucofan schist	metaarccosis metagrovac conglomerate	gneiss-micaschist	granulite	
Clay rocks	metapelite	phyllite (>20% sericite, <10% feld.) chlorite-epidote-chloritoid-phyllite albite-microcline-phyllite chloritoid garnet albite epidote chloritoidfels sericite	micaschist (>20% mica) muscovite-biotite-paragonite two micaceous shale stavorolite disthene garnet plagioclase microcline paragneiss (>20% feldspar) muscovitefels (>90% muscovite)	kinzigite pagnays garnet-sillimanite-cordierite-gnays granulite	
Bauxite		Korundum fels grindstone	sandpaper		

Marl	Glauco-phane schist	chlorite-fillite calcsilicaschist tremolite-phyllite epidote-amphibolite epidote-zoisite-calcphyllite garnet-epidote-amphibolite	kalksilikatfels paraamfibolite garnet-pyroxene-amphibolite hornblend-gnays diopsitfels	granulite	
Limestone	metacarbonate	marble partially tremolite chlorite and sericite	mica-marble garnet-marble		
Dolomite Quartz-sandstone Coal, bitumen	metacarbonate	dolomite-marble quartzite graphite	marble quartzite graphite		

**Table 3.1.** Changes in regional metamorphism facies of different types of rocks (simplified from the report of the symposium on the classification of metamorphic rocks-1962)

Metamorphism facies are mainly as follows:

- Zeolite
- Prehnite-pumpellyite
- Blueschist
- Greenschist
- Amphibolite
- Granulite
- Eclogite
- Albite-epidote hornfels
- Hornblend hornfels
- Pyroxene hornfels
- Sanidinite

Prehnite-pumpellyite and zeolite facies are grouped under the name of sub-greenschist facies in the current literature (Bucher and Frey, 1994).

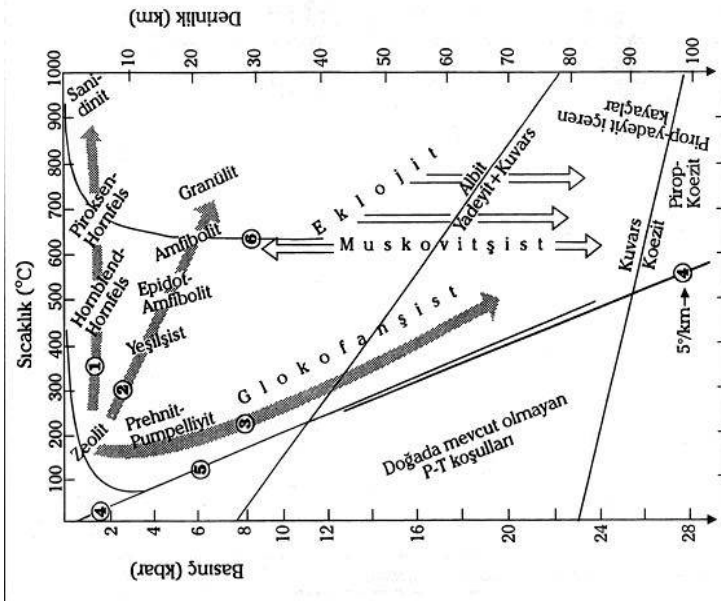


Figure 3.2. Location of metamorphic facies in the temperature and pressure diagram (Matthes, 1990)

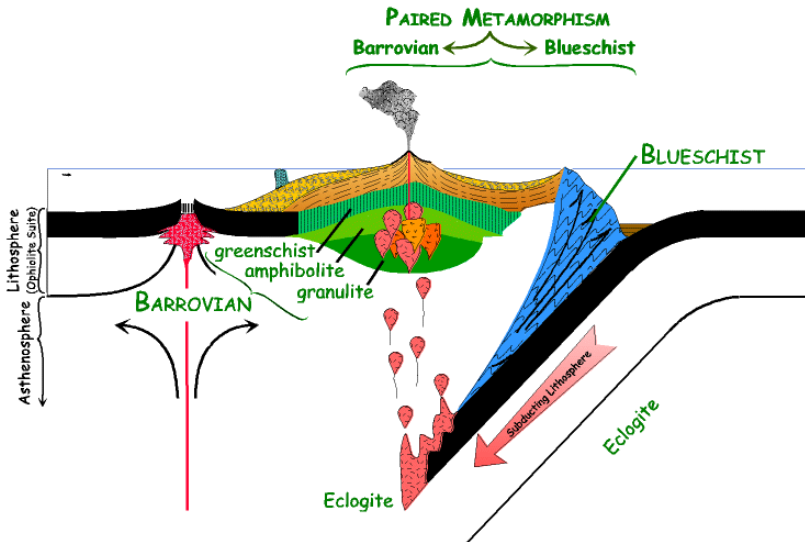
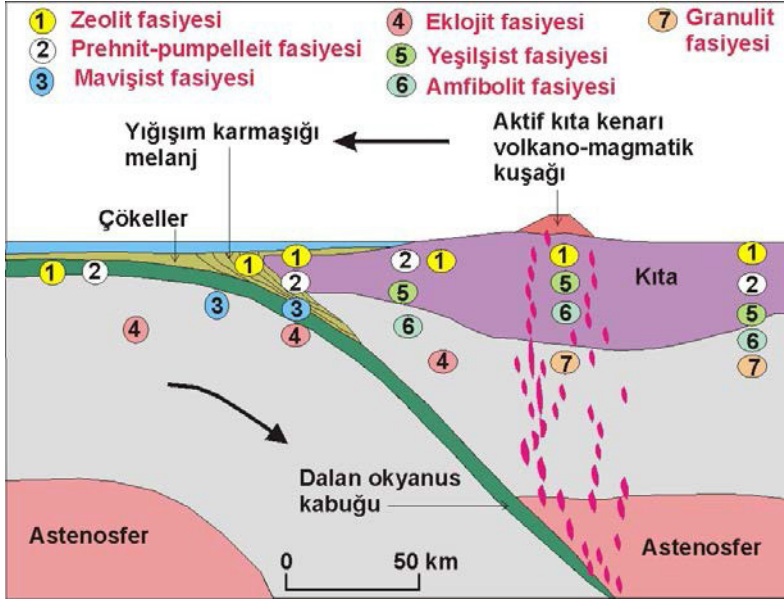


Figure 3.3. Location of metamorphic facies in subduction zones (<http-1>)



**Figure 3.4.** Location of metamorphic facies and partial melting of the lower crust and upper mantle due to pressure and temperature distribution at the boundary of continental crust and oceanic crust (Best, 1982)

### 3.1. Zeolite Facies

The zeolite facies characterizes the low temperature and pressure conditions with the zeolite group minerals lemontite and höyländite being typical minerals of this facies.

### 3.2. Prehnite-Pumpellyite Facies

As a result of the increase in temperature and especially pressure, the zeolite facies passes from the zeolite facies to the prehnite-pumpellyite facies. The typical minerals of this facies are prehnite and pumpellyite minerals.

### 3.3. Blueschist Facies

The Blueschist facies is characterized by high pressure and the same or slightly higher temperature conditions compared to the Prehnite-Pumpellyite and Zeolite facies. Typical minerals of this facies are glaucophane and lawsonite minerals. The name blueschist was given due to the presence of blue colored glaucophane and sodic amphiboles. In addition to glaucophane and lawsonite, disthene, epidote, zoisite, chlorite, garnet, phengite, chloritoid, paragonite, talc, jadeitic pyroxene, aragonite can

also be found. Feldspar and biotite are not found in this facies. Eskola also described this facies as glaucophane schist facies (Bucher and Grapes, 2015).

### **3.4. Greenschist Facies**

The Greenschist facies roughly includes rocks formed under low temperature (300-500 °C) and low-medium pressure conditions. The typical mineral assemblage of this facies is actinolite + chlorite + epidote + albite ± quartz. The first three minerals in this mineral assemblage are the minerals that give the rock its green color (Erkan, 2006).

### **3.5. Amphibolite Facies**

The typical minerals of the amphibolite facies, a regional metamorphism facies where pressure and temperature are high, are hornblende + plagioclase (anorthite content > 20%). Minerals such as staurolite, almandine, cordierite, andalusite, sillimanite, disthene, orthoclase are also found in rocks with suitable chemical composition (Erkan, 2006).

### **3.6. Granulite Facies**

The typical mineral assemblage of the granulite facies, represented by rocks formed under conditions of high temperature and high pressure, is augit + orthopyroxene + plagioclase, and Fe-Mg garnet minerals are also present. Since the rocks belonging to the granulite facies are almost dehydrated, these rocks were formed at low water pressure. If there is water in the environment, biotite and hornblende can also form in this facies depending on the formation conditions (Bucher and Grapes, 2015).

### **3.7. Eclogite Facies**

Eclogite facies rocks form over a wide range of temperatures and in different geodynamic environments (Bucher and Grapes, 2015). In addition, these rocks were formed under very high pressure due to their high density. Jadeite-rich clinopyroxene (omphacite) + pyrope-rich garnet minerals constitute the typical minerals of this facies. Depending on the temperature, if water is present in the environment, eclogites containing hornblende and glaucophane can also occur (Erkan, 2006). Eclogite facies rocks do not contain plagioclase.

The great majority of eclogites are found as tectonically transported blocks in chaotic melange zones in accretion zones in subduction zones

and in areas of blueschists, or in metamorphosed rocks of another facies (Bucher and Grapes, 2015)

### 3.8. Hornfels Facies

Contact metamorphism facies formed under low pressure can be grouped under the definition of hornfels facies. With the increase in temperature, these facies as;

- Albite - Epidote - Hornfels Facies
- Hornblend - Hornfels Facies
- Pyroxene - Hornfels Facies.

***Albite - Epidote - Hornfels Facies:*** This facies developed under low pressure and relatively low temperatures, taking its name from albite and epidote minerals. Hornfels is a rock formed by contact metamorphism. This facies is as follows;

In metabasites: albite + epidote + actinolite + chlorite + quartz

Metapelites are characterized by the minerals: muscovite + biotite + chlorite + quartz.

***Hornblende - Hornfels facies:*** This facies is characterized by low pressure but slightly higher temperatures, similar to the albite - epidote hornfels facies. Although it is named after the hornblende mineral, the appearance of this mineral is not limited to this facies. The Hornblend - Hornfels facies is as follows;

In metabasites: hornblende + plagioclase ± diopside, anthophyllite / cummingtonite, quartz

Metapelites are characterized by the minerals: muscovite + biotite + andalusite + cordierite + quartz + plagioclase.

***Pyroxene - Hornfels Facies:*** This facies is a contact metamorphism facies with high temperatures and named the presence of orthopyroxene similar to granulite facies. The Pyroxene-Hornfels facies as indicated by the following mineral assemblages;

In metabasites; orthopyroxene + clinopyroxene + plagioclase ± olivine or quartz

In metapelites; cordierite + quartz + sillimanite + K-feldspar (orthoclase) ± biotite ± garnet (If the temperature is below 750 °C, andalusite is found instead of sillimanite)

Carbonate rocks are characterized by the minerals calcite + forsterite ± diopside, periclase or diopside + grosular+ wollastonite ± vesuvianite (http-2).

### 3.9. Sanidinite Facies

Sanidinite facies rocks are formed under extremely high temperature and low pressure conditions. In this facies, the main mineral is sanidine and the typical rock is sanidinite. Also, depending on the rock of origin, the mineral assemblage can be tridymite, cordierite, wollastonite, diopside, anorthite. The sanidinite facies is a facies of contact metamorphism, which sometimes to the formation of rocks containing uncrystallized glassy material as a result of partial melting due to high temperature (http-3).

### 4. References

Best, M. G., 1982. *Igneous and Metamorphic Petrology*. San Francisco, 630 pp.

Bucher, K and Frey, M., 1994. *Petrogenesis of Metamorphic Rocks*. Springer, Berlin, 318 pp.

Bucher, K. and Grapes, R., 2015. *Petrogenesis of Metamorphic Rocks*. Springer, Berlin, 428 pp.

Erkan, Y., 2006. *Metamorphic Petrography*, TMMOB Chamber of Geological Engineering Publications, Ankara, 204 pp.

Eskola, P., 1915. On the relations between the chemical and mineralogical composition in the metamorphic rocks of the Orijarvi region, *Bulletin de la Commission geologique de Finlande*, 44, pp. 109-145.

http-1:<https://acikders.ankara.edu.tr/mod/resource/view.php?id=61033>

http-2: [https://en.wikipedia.org/wiki/Metamorphic\\_facies](https://en.wikipedia.org/wiki/Metamorphic_facies)

http-3:<https://terim.ahmetcadirci.com/yerbilim/sanidinit-fasiyesi.html>

Matthes S., 1990. *Mineralogie*, Springer-Verlag, Berlin Heidelberg.

Yardley, B. W. D., 1989. *An Introduction to Metamorphic Petrology*. Longman Earth Science Series, Singapore, 248 pp.

# CHAPTER 3

## INVESTIGATION OF TRAVERTINE CAVE STALAGMITES IN TAZEKENT VILLAGE (DİYADİN, AĞRI); ORIGIN AND CLIMATE INTERPRETATIONS

*Çetin YEŞİLOVA<sup>1</sup>*

*Erhan GÜLYÜZ<sup>2</sup>*

*Pelin Güngör YEŞİLOVA<sup>3</sup>*

*R. Burak TAYMUŞ<sup>4</sup>*

---

1 Doç. Dr., Yüzüncü Yıl University Department of Geological Engineering, 65080, VAN, TURKEY ORCID ID: 0000-0002-8884-0842, cetinyesilova@yyu.edu.tr

2 Doç. Dr., Yüzüncü Yıl University Department of Geological Engineering, 65080, VAN, TURKEY ORCID ID: 0000-0002-1539-7982, erhangulyuz@yyu.edu.tr

3 Doç. Dr., Yüzüncü Yıl University Department of Geological Engineering, 65080, VAN, TURKEY ORCID ID: 0000-0002-0748-6192, pelingungoriesilova@yyu.edu.tr

4 Dr Öğr. Üyesi., Yüzüncü Yıl University Department of Civil Engineering, 65080, VAN, TURKEY ORCID ID: 0000-0002-1489-9307, refikburaktaymus@yyu.edu.tr

## Introduction

Since speleothems are directly related to surface water chemistry, isotopic records obtained from such deposits and their precise dating are critically important both for the clarification of past climate records and the development of climate evolution models.

The fact that 70% of the data from a total of 500 caves in the world in the database of the Speleothem Isotopes Synthesis and Analysis Working Group (SISAL) is after 2007 and that data sets from only 2 caves in our country have been published is an indication that such records are currently popular but remain a “data gap” in terms of speleothem records in our own geography (Fig. 1).

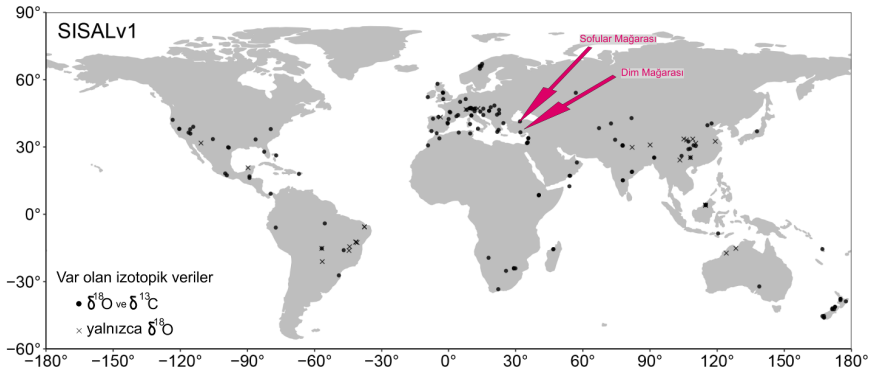


Figure 1. Geographic distribution of cave sedimentation records around the world according to the SISAL database (taken from Atsawawaranunt et al., 2018).

With this study, for the Eastern Anatolia Region, were presented a cave deposit precise climate data sets. Since this possible cave record model could be the first high-resolution and precise model for the region, it is thought that the project outputs could provide pioneering base data for studies to be conducted both globally and locally.

Eastern Anatolian climate records are limited (Çiner, 2003; Sarıkaya et al., 2011; Sarıkaya, 2012) and are mainly dependent on datasets from Lake Van and glacier records (Akçar and Schlücher, 2005). Datasets from the lake are related to sediment chemistry (Landmann et al., 1996a; Kadıoğlu et al., 1997; Çağatay et al., 2014; Stockhecke et al., 2014; Pickarski et al., 2015) and pollen records (Wick et al., 2003; Litt et al., 2014; Pickarski et al., 2015), while datasets from glaciers consist of cosmogenic ages of glacial valleys. Although the lake records are directly dependent on  $^{14}\text{C}$  or radiogenic dating of tephra levels in drillings (Mouralis et al., 2010; Sumita et al., 2012, Sumita and Schmincke, 2013a, 2013b, 2013c; Schmincke

et al., 2013), the historical resolution in these records is directly related to the error margins of the methods, sampling intervals and the potential of Lake Van, which is highly alkaline, to record climate records continuously. Composite analysis of drillings carried out in this lake shows an uninterrupted record for the last 90 thousand years (Stockhecke et al., 2014). However, the analysis of sediment samples taken from cores in terms of climate records does not indicate a single moment but gives the average of a certain time period and the age control of these data is again the product of a large-scale study (IODP). This study aims to detail the climate records presented on a large scale (roughly) for the region with high-resolution precise climate record analyses.

A limited number of cave sediment records have been added to the literature from our country (Sofular and Dim caves) (Fleitmann et al., 2009; Göktürk et al., 2011; Ünal-İmer et al., 2015). These records have been correlated with both global and local climate records and have been the basis for many studies, but one of these caves is on the Mediterranean coast while the other is on the Black Sea coast (Figure 1). The sediment to be studied within the scope of this study is located in the Eastern Anatolia region.

However, Micro-XRF scanning is widely used on lake/sea cores, but the application of this type of analysis on cave sediments is quite rare (e.g. Finne et al., 2015; Li et al., 2019; Scroxton et al., 2018) and these studies generally examined the distribution of a specific element in the sample. Within the scope of this study, it is anticipated that climate changes may directly affect the concentrations of elements in the cave sediment.

The aim of the study is to date a cave deposit for the first time in the Eastern Anatolia Region and partly in the Middle East with high resolution (U/Th method) and to present precise climate data sets for the age ranges to be obtained. Since this possible cave record model can be the first high resolution and precise model for the region, it is thought that the project outputs can provide pioneering base data for future studies both globally and locally. Within the scope of the project, micro-XRF analyses with 0.2 mm intervals were also performed on a stalagmite with the ITRAX core scanner device. As a result of this process, approximately 25 element data were obtained precisely from bottom to top. Such data sets for stalagmites are for certain elements in the literature and are very few in number (e.g. Finne et al., 2015; Li et al., 2019; Scroxton et al., 2018). Within the scope of the study, XRF data sets were tried to be correlated with both  $\delta^{18}\text{O}$  and  $\delta^{13}\text{C}$  records to be obtained within the scope of the project and global climate records. In case a consistent correlation is obtained, it is possible to add a new climate record variable to the literature through speleothems. In this case, it is considered as a secondary original value in addition to the contribution of the study to global and regional climate records.

## Geology

The Eastern Anatolian Region, which is the study area, has a compressional regime from the Upper Cretaceous to the present (Mc Kenzie, 1972; Le Pichon et al., 1973; Morelli, 1978). In the region, as a result of a tectonic regime of N-S compression and E-W extension, the crust shortened and rose (Şaroğlu and Yılmaz, 1984; Şaroğlu and Yılmaz, 1986). Many right and left lateral faults, opening cracks and thrusts occurred as a result of this tectonic regime (Şaroğlu and Yılmaz, 1984). These faults, which developed parallel to the Eastern Anatolian fault zone, are the most characteristic features of the Eastern Anatolian compressional zone (Bozkurt, 2001; Eren, 2009).

Tazekent Travertines are located within the Eastern Anatolian plateau. The plateau; It developed as a product of the compression (continent-continent collision) regime that started 19 million years ago (Gülyüz et al., 2019). The basin took its final shape with effective volcanism, which was one of the results of this compression regime. With this developing regime, many paleo and active faults developed in the basin (Şaroğlu and Yılmaz, 1986; Koçyiğit, 2013). As a result of all these, many travertine formations have occurred in the basin and continue to occur. When the geology of the study area is examined, metamorphic, magmatic and sedimentary units are observed. All these units have been defined, mapped and explained in detail (Aslan et al., 1991; Burcak et al., 1997; Zaman et al., 2000; Pasvanoğlu and Guler, 2010; Coban, 2011; Colakoğlu et al., 2011; Mutlu et al., 2013; Pasvanoğlu, 2013; Sürmeli and Mesci, 2014; Kardaş and Köse, 2019; Kıyadeh and Köse, 2019).

The basement of the region is formed by Eocene-Miocene clastic rocks and limestones. Volcanics deposited from Upper Miocene to Quaternary unconformably overlie these clastic and carbonate rocks (Fig. 2). Travertines formed due to fractures developed in the region unconformably cover all these units (Fig. 3). The study area ends with alluviums that have continued to form from the Quaternary to the present (Aslan et al., 1991; Burcak et al., 1997; Zaman et al., 2000; Pasvanoğlu and Guler, 2010; Coban, 2011; Colakoğlu et al., 2011; Mutlu et al., 2013; Pasvanoğlu, 2013; Sürmeli and Mesci, 2014; Kardaş and Köse, 2019; Kıyadeh and Köse, 2019).

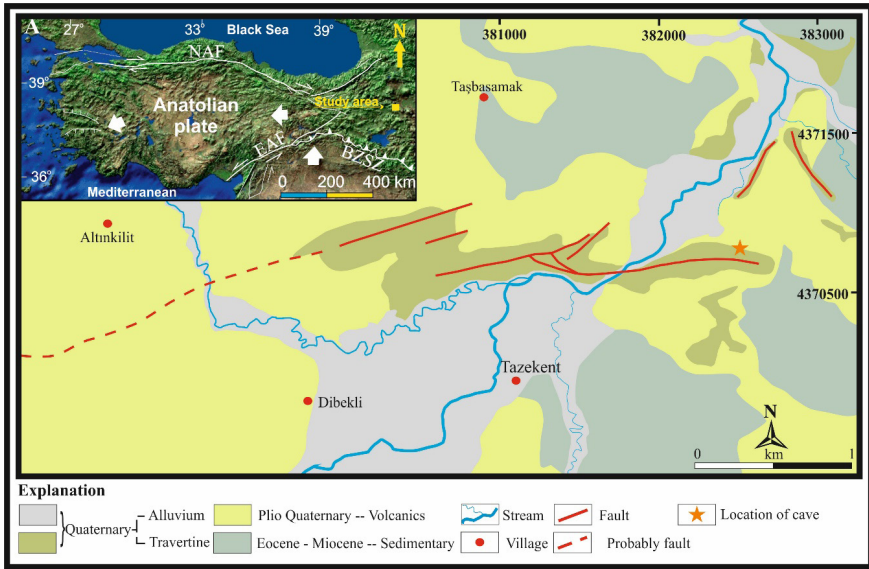


Figure 2. Geological map of the study (Modified from, Yeşilova and Yeğen 2025).



Figure 3. Different type travertine formations observed in the region. A-D, ridge type travertine, B, sheet type travertine and C, dome type travertine formations.

## Materials and Methods

In the study, the materials and method can be grouped under 3 separate headings. These headings cover sampling, field studies, and ITRAX

micro-XRF analyses, respectively. Figure 4 shows the location of the study area and the processes of sticking and cutting the stalagmite and the aftermath.

### ***Sampling:***

This process is now complete and is independent of the project proposal. The location of the stalagmite sample and the cross-section of the cave (vertical cleft) where it was previously located are presented in Figure 5. The stalagmite sample to be analyzed within the scope of the project was found in 3 pieces in the field. This sample was combined with glue and made into a whole with a loss of approximately 3 cm in the vertical. The whole sample was placed in a longitudinal mold and fixed with concrete to make it ready for vertical and horizontal cutting (Fig. 4C-E). The cutting process of the sample was carried out with a diamond-tipped saw rotating at a constant speed under constant flow water in a marble production facility in Van, and the records that could be gained by heating the sample during cutting were kept at a minimum level (Fig. 4F-H).

### ***Field Studies:***

During the field studies, the geological units in the cave where the stalagmite was located and its surroundings were identified, and the lithofacies and lithodemic features of these units were determined. Following these studies, a 1/25000 geological map of the region was prepared and the structural elements were transferred to the map (see Fig. 2). After these studies were completed, the studies inside the cave were started. The location and position of the stalagmite removed from the cave were determined exactly (for the accuracy of this process, the lowest surface of the stalagmite was kept as a whole) (Fig. 5). Another study planned to be conducted in connection with the study is to take hand samples from the rock assemblages (generally Quaternary-aged travertine according to current maps) that crop out around the cave. The reason for such a study is to investigate whether the origins of the relevant distributions are related to the wall rocks in the event that the element ratio distributions to be obtained systematically from the stalagmite within the scope of the study cannot be directly associated with climate changes.



Figure 4. A) Basic structural elements of the Eastern Anatolian geological map (modified from MTA 2002 and Okay and Tüysüz, 1999), note: Red box shows the sample location, B) GoogleEarth screenshot shows the sample point, C) Stalagmite image found in 3 pieces, D) Whole stalagmite image joined with glue, E) Stalagmite image taken in concrete mold, F) Stalagmite image cut at constant water flow and constant speed, G) Stalagmite vertical section image, H) Stalagmite horizontal section image.

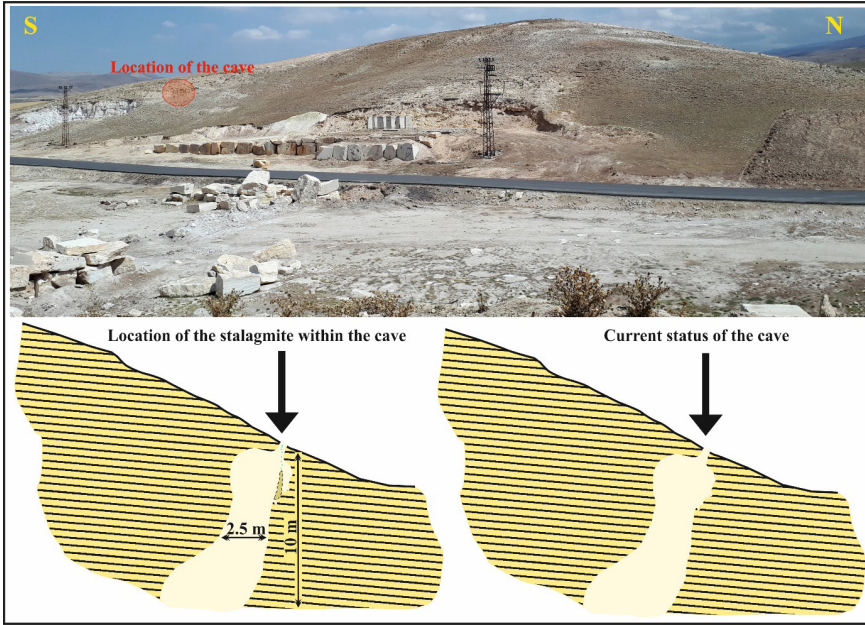


Figure 5. The location of the stalagmite found in pieces in the cave and the location of the stalagmite in the cave (the section of the cave is drawn in the W-E direction). Note 1: The stalagmite found in the cave is only 5 meters inside the crevice mouth, and no water/water dripping is currently observed in the cave. This shows that the stalagmite growth occurred before today (before the crevice mouth was formed) but at a location very close to the surface, indicating that the possible effects inside the cave have a minimum effect on the climate record. Note 2: The location where the stalagmite emerged in the cave is visible and known.

#### ***ITRAX micro-XRF analyses:***

This process is planned to be performed with the ITRAX micro-XRF device. This process consists of 7 stages; (i) checking whether the equipment is working properly, (ii) sample preparation (this process is complete), (iii) placing the sample in the holder, (iv) scanning the sample surface and creating a 3D map of the sample surface area before measurement, (v) taking X-ray radiography images, (vi) determining the XRF scanning parameters (resolution - it is planned to scan the project samples with 0.2 mm sensitivity), (vii) obtaining the analysis results and obtaining visual outputs. As can be seen in Figure 4G, the growth axis of the stalagmite is not a single straight line. Obtaining accurate and complete results depends on scanning along as many overlapping axes as possible. Therefore, it is thought that approximately seven times the total length of the stalagmite may be needed to scan, which corresponds to a total of approximately 10

m (7x1.4) micro-XRF scan at 0.2 mm resolution. The reason for wanting to scan on different lines of this type is to control possible changes/anomalies on the sample multiple times. As a result of all processes, the density distribution of 25 different elements along the sample lines will be obtained and these data sets will be used in paleoclimatic modeling/correlations. The study by Scroxton et al. (2018) provides a good example of how the dataset to be obtained from ITRAX within the scope of the proposed project can be used in paleoclimate interpretations. In addition to stable Oxygen and Carbon isotope ratios, the use of trace element ratios such as Mg/Ca and Sr/Ca is increasing day by day in order to obtain paleoclimate records from stalactites and stalagmites. Scroxton et al. (2018) clearly illustrated (Figure 6A). In Figure 6B, Scroxton et al. (2018) compare the Sr/Ca record obtained with the ITRAX scan with the paleoclimate record obtained by Griffiths et al. (2016) based on isotope data and trace element measurements. As can be seen, the Sr/Ca graph obtained with ITRAX is quite similar to the paleoclimate record. Roughly, it can be said that dry periods are represented by high Sr/Ca values. With the proposed project, it is planned to obtain results similar to the study of Scroxton et al. (2018), and thus to contribute to the literature that high-resolution core scanners can also be used advantageously in stalactite-stalagmite paleoclimate studies.

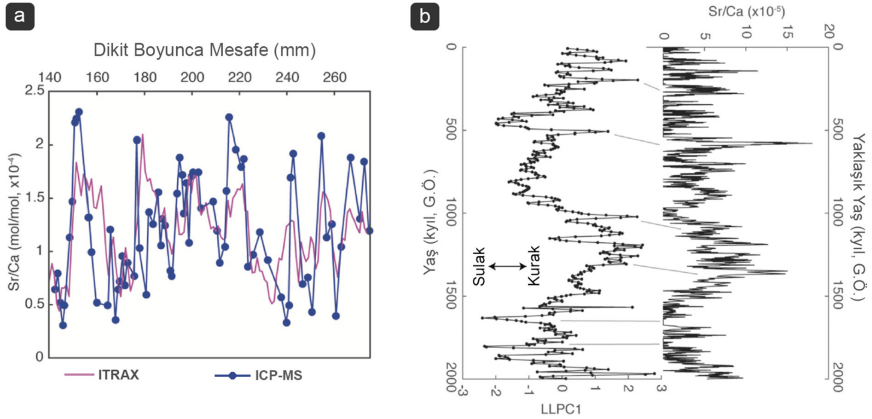
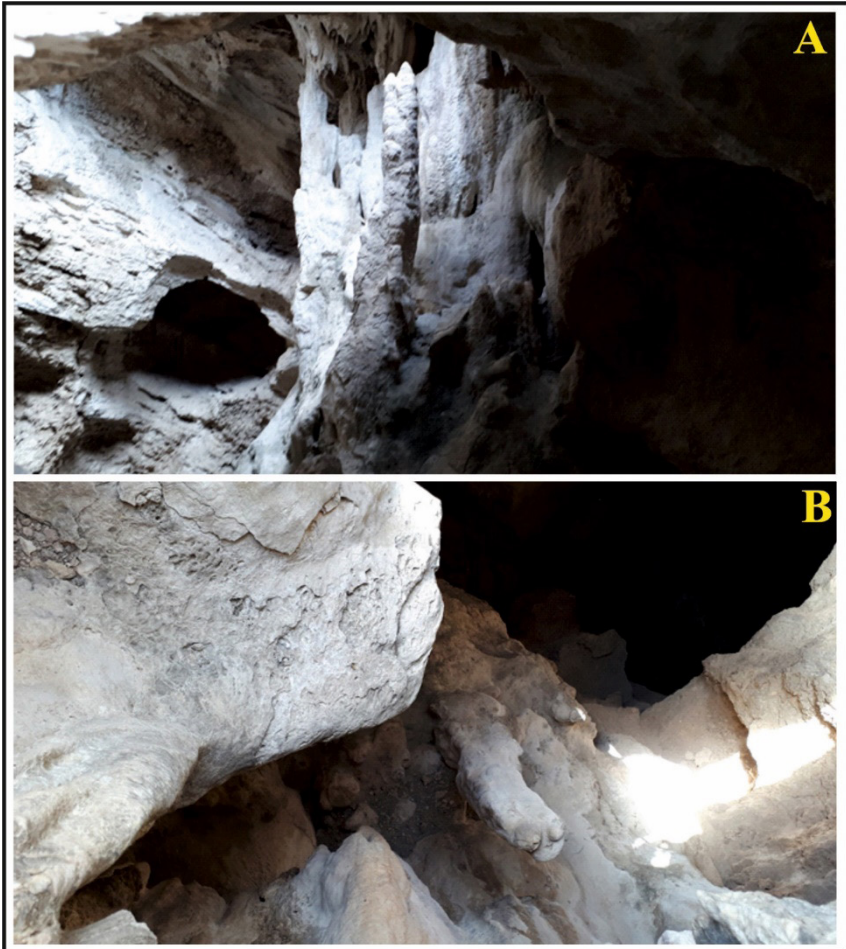


Figure 6. A) Comparison of Sr/Ca values obtained with the IITRAX micro-XRF scanner along the stalagmite examined by Scroxton et al. (2018) with those obtained with ICP-MS. B) Comparison of the Sr/Ca graph obtained by Scroxton et al. (2018) with the paleoclimate record (LLPC1) obtained by Griffiths et al. (2016) based on isotope data and trace element measurements.

## **Result**

### ***Travertines and the status of the cave***

The cave where the stalagmite is located is located on the northern slope of the travertines located in the north-northeast of Tazekent village. This cave, which has an average depth of 10 m and a width of 2.5 m, has grown vertically (see Fig. 5, Fig. 7). There are several studies on travertines (Sürmeli and Mesci, 2014; Yeğen, 2021; Yeşilova and Yeğen, 2024). In the travertine system of Tazekent Village, travertines were formed by opening cracks in the N 50 E and N 80 E directions and waters coming to the surface from these cracks (Yeğen 2021). In the main crack forming the travertines, an average of 150 cm thick vertical and symmetrical travertine formation was observed. The travertine thickness around the crack is 240 m. The opening crack on the travertines whose formation is completed can be clearly observed (Yeğen 2021). Sürmeli and Mesci (2014), in their study on the tectonic development of the ridge-type travertines in the region, determined ages between 125 - 10 ka. The samples taken were taken symmetrically from the samples that were upright in the opening crack (crack filling).



*Figure 7. A) Side view of the cave and B) top view.*

Again, Sürmeli and Mesci (2014) stated that it was in the NE-SW direction and the opening speed was between 1.05 - 0.012 mm/year, and the average speed was 0.352 mm/year. Yeğen 2021 dated the travertines in his master's thesis. He made the mentioned datings from the travertine wing. In his study, he took samples from a position close to the foundation, the middle and the top point of the Tazekent Village travertines. In the analysis results, ages of 215.16 - 118.40 - 31.44 ka were obtained. Since the sample taken from the bottom did not represent the lowest point of the travertines, it was stated that the travertines could be even older.

In their study conducted in 2024, Yeşilova and Yeğen divided the Tazekent Village Travertines into 7 facies (Fig. 8). These facies are;

1. Brecciated-lithoclastic facies,

2. Crystalline crust facies,
3. Shrub type facies,
4. Raft type facies,
5. Stromatolithic facies,
6. pubble gas facies,
7. Paleosoil facies.

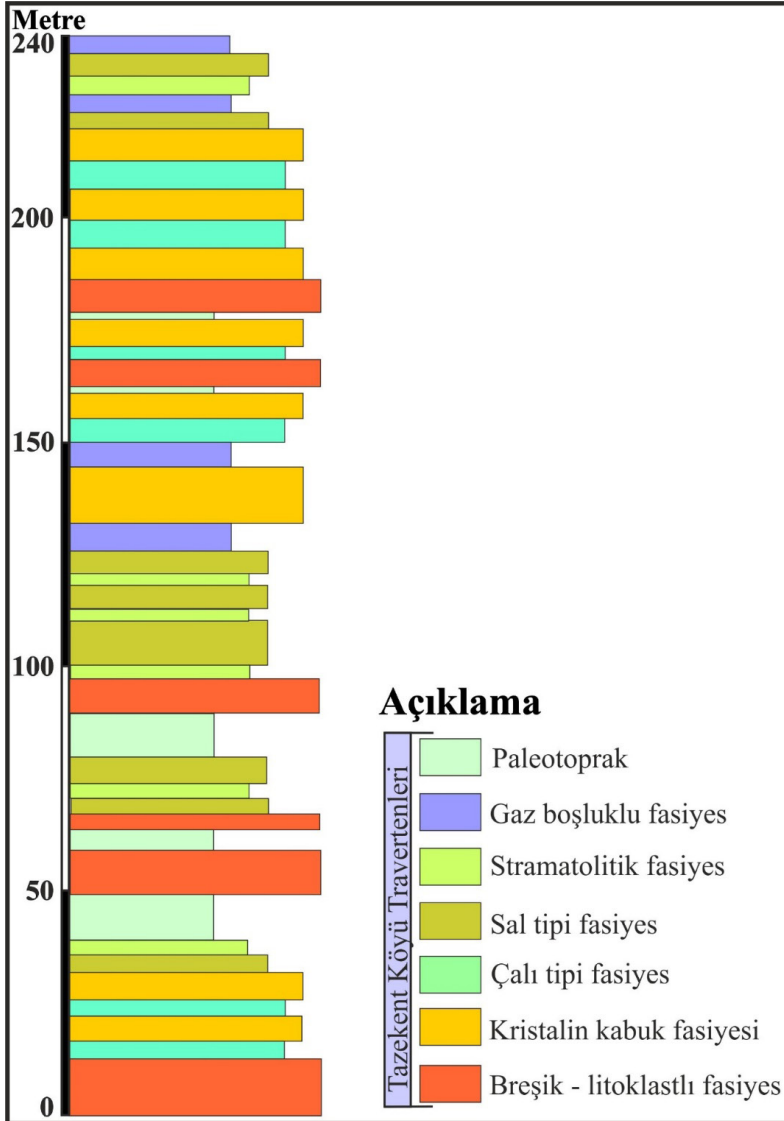


Figure 8. Column section of travertines (taken from Yeşilova Yeğen, 2025).

## Mikro XRF

The stalagmite in question was first cut in half and then a 5 cm thick slice was cut (Figure 9). Since the stalagmite did not develop in a perfect linearity, its stratigraphy was carefully examined and 8 sections were prepared for ITRAX scans, which would partially overlap each other stratigraphically and cover the entire stratigraphy of the stalagmite (Figure 9). ITRAX scans were performed at the MTA Marine Research Department Laboratory using a Molybdenum tube with a measurement time of 5 seconds every 0.5 mm. As a result of the measurements, a geochemical data set of 161.6 cm in length covering 18 elements (Al, Si, S, Cl, Ca, Ti, Cr, Mn, Fe, Ni, Cu, Zn, As, Br, Sr, Zr, Ba and Pb) was obtained (Table 1). In Figure 9, only the profiles of Ca and Sr elements from the data set are shown next to the optical images of the stalagmite sections. There are many anomalies along the profiles that are likely to be related to ancient climate conditions. In order to reveal the geochemical paleoclimate record recorded along the stalagmite, first of all, the overlapping parts of the 8 sections must be carefully correlated to obtain an integrated geochemical record.

*Table 1. A small part of the Micro XRF results performed on stalagmite.*

Al	Si	S	Cl	Ca	Ti	Cr	Mn	Fe	Ni	Cu	Zn	As	Br	Sr	Zr	Pb
20	0	327	111	241158	38	29	49	439	313	0	137	0	36	4165	182	50
33	14	267	90	218486	30	0	19	753	278	24	125	130	71	5007	172	0
20	78	250	88	255913	72	0	41	832	452	0	195	74	77	5607	50	0
0	0	240	89	256078	51	11	90	267	465	20	57	0	23	5154	105	273
49	0	212	153	267459	11	11	34	180	382	4	198	0	56	5323	152	119
9	5	296	217	256672	10	4	54	160	438	9	105	54	55	5566	114	0
27	0	249	264	258101	11	0	34	189	456	0	253	0	160	5692	231	217
7	5	135	126	246379	12	0	162	219	432	19	79	0	5	5569	178	170
23	0	214	161	257375	10	50	104	234	450	0	123	0	95	6074	211	95
23	0	176	162	223879	27	12	10	375	318	21	187	0	70	5182	103	122
28	0	203	145	278031	25	0	97	165	455	13	94	0	39	5057	82	181
0	0	123	20	273459	0	9	104	127	511	0	78	0	47	5957	122	172
42	9	193	77	274136	16	0	111	149	518	0	60	0	98	5917	127	231
8	0	84	51	275160	17	0	130	104	593	10	17	0	39	6085	110	191
16	0	141	20	276124	27	6	127	160	565	0	77	0	120	5912	92	181

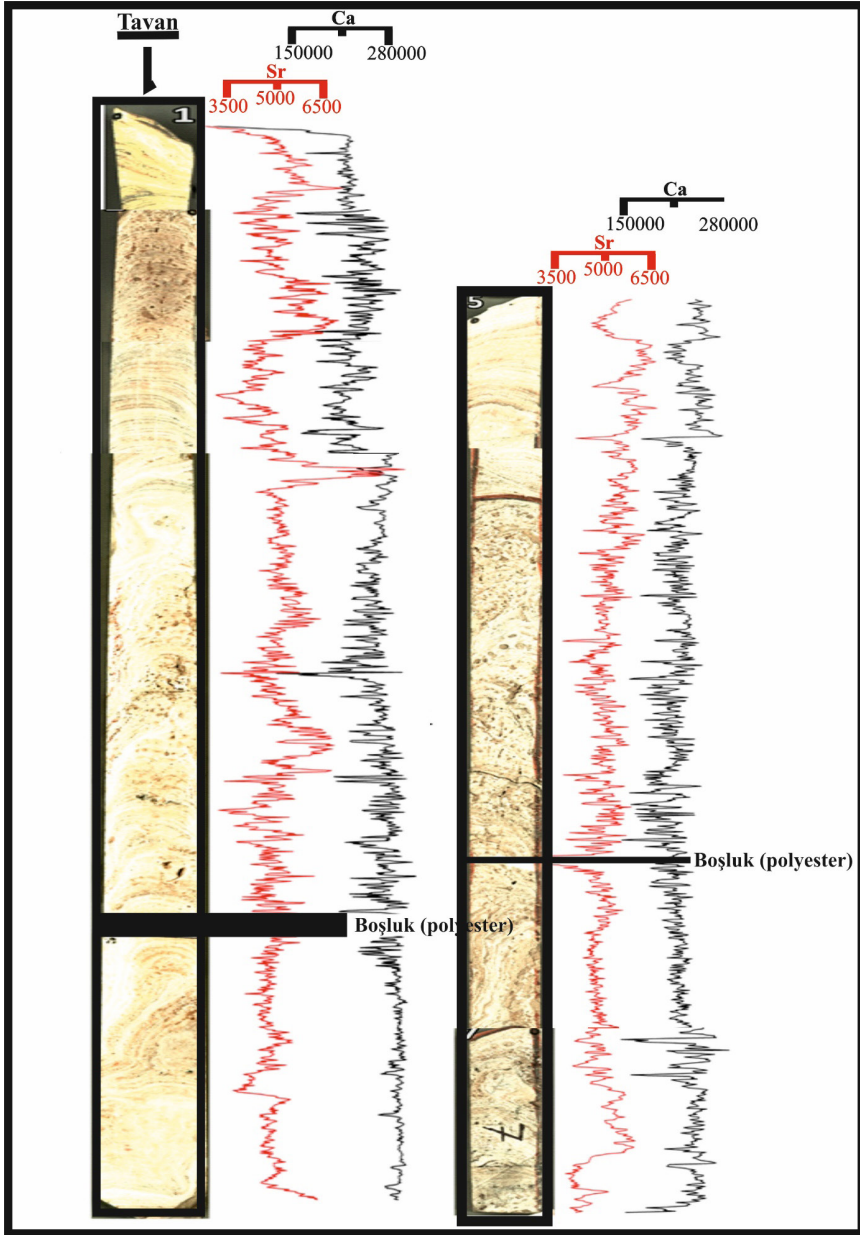


Figure 9. Sr/Ca Micro XRF values of the entire stalagmite.

## Discussion and Conclusion

As a result of the field studies, similar results were obtained as in the Yeğen, 2021 study. In this context, it was determined that the Tazekent Village Travertines morphologically showed dome and ridge type formation. Again, the Tazekent Village Travertines were divided into 7 facies:

1. Brecciated-lithoclastic facies,
2. Crystalline crust facies,
3. Shrub type facies,
4. Raft type facies,
5. Stromatolithic facies,
6. Gas cavity facies,
7. Paleosoil facies.

According to these facies obtained; The stromatolites in the study area indicate that lacustrine areas that will create living activity on the travertines have developed. The growth of these stromatolites in a continuously upward growing system shows that the current lake level is constantly rising (Martin-Bello et al., 2019). Again, the fissures and karstic spaces indicate that the opening continues, and the raft-type facies developing in these areas indicate travertine deposition. The fact that the crystalline crustal facies consists of clear calcites and fans of equal length indicates that this crust was formed in the source area and in the slope environment (Özkul et al. 2001; Barilaro et al. 2011). The block-size material observed in the brecciated-lithoclastic facies indicates that they were not transported and were deposited right at the bottom of the place where they were broken off. Both the fractured and cracked structure, the raft-type facies filling these structures, the lacustrine areas formed on the distant slopes of the travertines and the gravel content of the brecciated-lithoclastic facies indicate that not only volcanism but also tectonism occurred intensively during the formation of the travertines (Gradziński., 2010).

The changes in the values of the elements obtained as a result of the Micro XRF analysis performed on the stalagmite are used in the interpretation of many data such as climate, diagenesis, volcanism (Croudace et al., 2006; Rothwell and Croudace, 2015) (Table 1, Appendix-1). The sudden Cu increases obtained along the plane where the Micro XRF analysis was performed indicate diagenetic mobility, however, the high Mn levels observed together with copper confirm this situation (Croudace et al., 2006; Rothwell and Croudace, 2015). The decrease in the Mn level indicates the decrease in the groundwater level (Croudace et al., 2006; Rothwell and

Croudace, 2015). The climate data are processed into the analysis results in Figure 10.

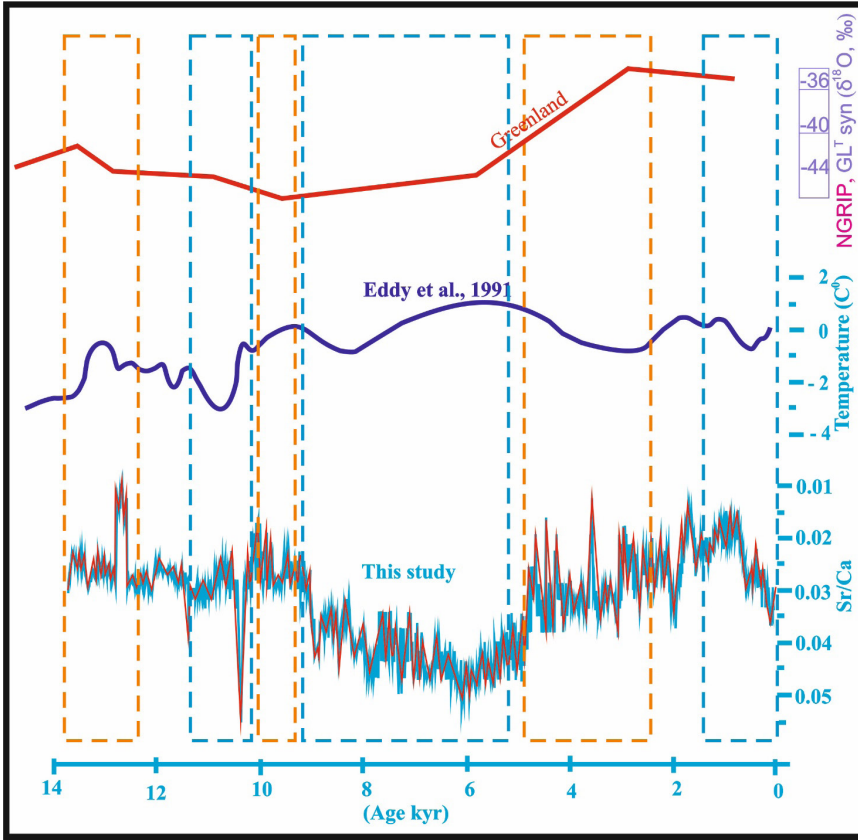


Figure 10. Sr/Ca values obtained from micro XRF studies and comparison of these values with NGRIP data and climate data of Eddy et al., 1991. Orange dashed boxes indicate warm periods, Blue dashed boxes indicate cold periods.

Again, Zr values obtained from the analysis results indicate volcanic activity during the formation of the stalagmite. This situation was also stated in the study conducted by Yeşilova and Yeğen 2025. In addition to all these, Sr/Ca values observed along the section indicate dry and rainy times (see Fig 9 - 10). In Figure 13, Sr/Ca values obtained from stalactites are compared with NGRIP data and Eddy et al. (1991) climate data. According to the correlation, 3 warm periods and 3 cold periods were observed during the development of the stalagmite. It was observed that the obtained data are compatible with other climate studies. The study needs to be reinforced with age data.

**Acknowledgements.** This study was supported by Yüzüncü Yıl University Scientific Research Project Council (YYÜ, BAP, Project No: FBA-2020-9007).

## REFERENCES

- Akçar, N. and C. Schlüchter, 2005. "Paleoglaciations in Anatolia: A schematic review and first results". *Eiszeitalter und Gegenwart*. 55, 102–121
- Aslan, Ö., Erkanol, D., Burçak, M., Avşar, M., Kocaman, H., 1991. 1/100.000 Ölçekli Sayısal Jeoloji Haritası Doğubayazıt J51 Paftası. Türkiye Jeoloji Veri Tabanı, Jeoloji Etütleri Dairesi Başkanlığı, Maden Tetkik ve Arama Genel Müdürlüğü, Ankara.
- Burçak, M., Yıldırım, T., Yücel, M., 1997. Ağrı-Diyadin-Çermik Sahası Jeotermal- Jeofizik Etüt Raporu (yayınlanmamış). MTA Der. Rap., 10020, Ankara. 12.
- Bozkurt, E., 2001, Neotectonics of Turkey-a Synthesis. *Geodinamica Acta* 14: p:3-30.
- Croudace, I.W., Rindby, A., Rothwell, R.G. 2006. ITRAX: description and evaluation of a new multifunction X-ray core scanner. In: Rothwell R.G. (ed) *New techniques in sediment core analysis*. *Geol Soc Spec Publ* 267:51–63.
- Çağatay, M.N.**, Öğretmen, N., Damcı, E., Stockhecke, M., Sancar, Ü., Eriş, K.K., Özeren, S., 2014. «Lake level and climate records of the last 90 ka from the Northern Basin of Lake Van, eastern Turkey». *Quaternary Science Reviews*. 104, 97–116.
- Çiner A (2003). «Recent glaciers and late quaternary glacial deposits of Turkey». *Geological Bulletin of Turkey* 46 : 55–78.
- Çoban, A., 2011. Diyadin (Ağrı) ve Yakın Çevresinde Jeomorfolojik Birimler ile Arazi Kullanımı Arasındaki İlişkiler (Yüksek Lisans Tezi). Yüzüncü Yıl Üniversitesi, Sosyal Bilimler Enstitüsü, Van.
- Çolakoğlu, A.R., Oruç, M., Arehart, G.B., Poulson, S., 2011. Geology and isotope geochemistry (C-O-S) of the Diyadin gold deposit, Eastern Turkey: a newly discovered carlin-like deposit. *Ore Geology Reviews*, 40: 27-40.
- Eddy, J.A., OIES., Bradley, R.S., 1991. University of Massachusetts, Earthquest, Spring
- Eren, Y., 2009. Neotektonik Ders Notları. <http://www.yasareren.com/yasareren/pdfdosy/neotektonik/Microsoft%20Word%20-%20neotektonikdersnotu.pdf>. T.C.Selçuk Üniversitesi, Mühendislik-Mimarlık Fakültesi, Jeoloji Mühendisliği Bölümü, Konya. Erişim Tarihi: 28.07.2018.
- Fairchild I., Smith C. L., Baker A., Fuller L., Spötl Ch., Matthey D., Mc Dermott F. & E.I.M.F., 2006. "Modification and preservation of environmental signals in speleothems". *Earth-Science Reviews*, 75, 1-4, 105–153.
- Finné M, Kylander M, Boyd M, Sundqvist H, Löwemark L. 2015. "Can XRF scanning of speleothems be used as a non-destructive method to identify paleoflood events in caves? Inter". *J Speleol*, 44: 17–23
- Fleitmann, D., Cheng, H., Badertscher, S., Edwards, R.L., Mudelsee, M., Göktür O.M., Fankhauser, A., Pickering, R., Raible, C.C., Matter, A., 2009. "Ti-

ming and 560 climatic impact of greenland interstadials recorded in stalagmites from northern 561 Turkey”. *Geophysical Research Letters* 36.

- Göktürk, O.M.; Fleitmann, D.; Badertscher, S.; Cheng, H.; Edwards, R.L.; Leuenberger, M.; Fankhauser, A.; Tüysüz, O.; Kramers, J. 2011. “Climate on the southern Black Sea coast during the Holocene: Implications from the Sofular Cave record”. *Quat. Sci. Rev.* 30: 2433–2445.
- Griffiths, M.L., Kimbrough, A.K., Gagan, M.K., Drysdale, R.N., Cole, J.E., Johnson, K.R., Zhao, J.-X., Cook, B.I., Hellstrom, J.C., Hantoro, W.S., 2016. “Western Pacific hydroclimate linked to global climate variability over the past two millennia”. *Nat. Commun.* 7. <http://dx.doi.org/10.1038/ncomms11719>.
- Gülyüz, E., Özkaptan, M., Kaymakci, N., Persano, C., Stuart, F. M., 2019. Kinematic and thermal evolution of the Haymana Basin, a fore-arc to foreland basin in Central Anatolia (Turkey). *Tectonophysics*, **766**: 326-339.
- Hendy C.H., 1971. “The isotopic geochemistry of speleothems - I. The calculation of the effects of different modes of formation on the isotopic composition of speleothems and their applicability as palaeoclimatic indicators”. *Geochim. Cosmochim. Acta*, 35: 801–824.
- Kadioğlu, M., Şen, Z., Batur, E., 1997. “The greatest soda-water lake in the world and how it is influenced by climatic change”. *Annu. Geophys.* 15, 1489–1497.
- Kardaş, S., 2019. Diyardin (Ağrı) Kuzeyinin Tektonik Özellikleri ve Jeotermal Potansiyeli (Yüksek Lisans Tezi). Van Yüzüncü Yıl Üniversitesi, Fen Bilimleri Enstitüsü, Van.
- Kıyadeh, A.A.H., 2019. Diyardin (Ağrı) Güneyinin Tektonik Özellikleri ve Jeotermal Potansiyeli (Yüksek Lisans Tezi). Van Yüzüncü Yıl Üniversitesi, Fen Bilimleri Enstitüsü, Van.
- Koçyiğit, A., 2013. New Field And Seismic Data About The İntraplate Strike-Sli Deformation İn Van Region. East Anatolian Plateau. E. Turkey. Middle East Technical University. Department of Geological Engineering. Active Tectonics and Earthquake Research Lab.. TR-06800 Ankara. Turkey.
- Landmann, G., Reimer, A., Lemcke, G., Kempe, S., 1996a. “Dating Late Glacial abrupt climate changes in the 14,570 yr long continuous varve record of Lake Van, Turkey”. *Palaeogeogr. Palaeoclimatol. Palaeoecol.* 122, 107–118.
- Le Pichon, X., Francheteau, J., Bonnin, J., 1973. *Plate Tectonics: Developments in Geotectonics*. 6. Elsevier Science Ltd., Amsterdam. 300.
- Li, D., Tan, L., Guo, F. et al. 2019. “Application of Avaatech X-ray fluorescence core-scanning in Sr/Ca analysis of speleothems”. *Science China Earth Sciences*, 62: 964-973.

- Litt, T., Pickarski, N., Heumann, G., 2014. "A 600,000 Year Long Continental Pollen Record from Lake Van, Eastern Anatolia (Turkey)". *Quat. Sci. Rev.* 104, 30 - 41.
- McKenzie, D.P., 1972. Active tectonics of Mediterranean region, *Geophys. J.R., Ast. Soc.*, 30: 109-185.
- Morelli, C., 1978. Eastern Mediterranean: geophysical results and implications. *Tectonophysics*, 46: 333-346
- Mouralis, D., Kuzucuoğlu, C., Scaillet, S., Doğu, A.F., Christol, A., Akköprü, E., Fontugne, M., Zorer, H., Guillou, H., 2010. "Les pyroclastites du sudouest du lac de Van (Anatolie orientale, Turquie): implications sur la paléo-hydrographie régionale". *Quaternaire*. 21, 417-433.
- Mutlu, H., Aydın, H., Kazancı, A., 2013. Diyadin (Ağrı) jeotermal sahasına yönelik jeokimyasal ve izotopik bulgular. 11. Ulusal Tesisat Mühendisliği Kongresi Jeotermal Enerji Semineri. 17-20 Nisan 2013, İzmir. 47-67.
- Pasvanoğlu, S., Güler, S., 2010. Hydrogeological and geothermal features of hot and mineralized waters of the Ağrı- Diyadin (Turkey). *Proceedings World Geothermal Congress*. 25-29 April 2010, Bali, Indonesia. 1-10.
- Pasvanoğlu, S., 2013. Hydrogeochemistry of thermal and mineralized waters in the Diyadin (Ağrı) area, Eastern Turkey. *Applied Geochemistry*, 38: 70-81.
- Pentecost A (2005). "Travertine". Berlin, Germany: Springer.
- Pickarski, N., Kwiecien, O., Langgut, D., Litt, T., 2015. "Abrupt climate and vegetation variability of eastern Anatolia during the last glacial. *Climate of the Past*". 11, 1491 - 1505.
- Rothwell, R.G., Croudace, I.W. 2015. Twenty years of XRF core scanning marine sediments: What do geochemical proxies tell us? In, Croudace, I.W. and Rothwell, R.G, (eds.) *Micro-XRF Studies of Sediment Cores: Applications of a non-destructive tool for the environmental sciences*. Dordrecht, NL. Springer, pp. 25-102. (Developments in Paleoenvironmental Research, 17).
- Sarıkaya M, Çiner A, Zreda M (2011). "Quaternary glaciations of Turkey. In: Ehlers J, Gibbard P, Hughes P, editors. *Quaternary Glaciations - Extent and Chronology*". Oxford, UK: Jordan Hill, pp. 393-403.
- Sarıkaya MA (2012). "Recession of the ice cap on Mount Ağrı (Ararat), Turkey, from 1976 to 2011 and its climatic significance". *J Asian Earth Sci* 46: 190-194.
- Schmincke, H.U., Sumita, M., Paleovan scientific team, 2013. "Impact of volcanism on the evolution of Lake Van III: Incekaya - an exceptionally large magnitude (DRE > 1 km<sup>3</sup>) subaqueous/subaerial explosive basaltic eruption". Abstract Presented at DFG IODP/ICDP Kolloquium, Freiburg, Germany.

- Schwarcz, H.P., (1986). "Geochronology and isotopic geochemistry of speleothems". Fritz, P., Fontes, J.C. Handbook of Environmental Isotope Geochemistry Elsevier, Amsterdam.271–300
- Schwarcz, H.P. 1989. "Uranium series dating of Quaternary deposits". Quaternary International 1: 7-17.
- Schwarcz, Henry P., 2005. "Uranium series dating in paleoanthropology". Evolutionary Anthropology: Issues, News, and Reviews. 1 (2): 56–62*
- Scroxtton N, Burns S, Dawson P, Rhodes J M, Brent K, McGee D, Heijnis H, Gadd P, Hantoro W, Gagan M. 2018. "Rapid measurement of strontium in speleothems using core-scanning micro X-ray fluorescence". Chem Geol, 487: 12–22
- Sharp Z. 2007. "Principles of stable isotope geochemistry. Pearson Education, Inc., Upper Saddle River", NJ 07458, 344 p.
- Shen, C.-C., Cheng, H., Edwards, R.L., Moran, S.B., Edmonds, H.N., Hoff, J.A., Thomas, R.B., 2003. "Measurement of attogram quantities of  $^{231}\text{Pa}$  in dissolved and particulate fractions of seawater by isotope dilution thermal ionization mass spectroscopy". Analytical Chemistry. 75, 1075–1079.
- Shen, C.-C., Wu, C.-C., Cheng, H., Edwards, R.L., Hsieh, Y.-T., Gallet, S., Chang, C.-C., Li, T.- Y., Lam, D.D., Kano, A., Hori, M., Spötl, C., 2012. "High-precision and high-resolution carbonate  $^{230}\text{Th}$  dating by MC-ICP-MS with SEM protocols". Geochimica et Cosmochimica Acta. 99, 71–86.
- Stockhecke, M., Sturm, M., Brunner, I., Schmincke, H.U., Sumita, M., Kipfer, R., Çukur, D., Kwiecien, Anselmetti, F.S., 2014. "Sedimentary evolution and environmental history of Lake Van (Turkey) over the past 600,000 years". Sedimentology. 61, 1830-1861.
- Sumita, M., Schmincke, H.-U., "Paleovan scientific team, 2012. The climatic, volcanic and geodynamic evolution of the Lake Van-Nemrut-Süphan system (Anatolia) over the past ca. 550-600 000 years. A progress report based on a study of the products of explosive volcanism on land and in the lake". In: Extended Abstract Presented at IODP/ICDP Kolloquium, Kiel, Germany, pp. 157-162.
- Sumita, M., Schmincke, H.U., 2013a. „Impact of volcanism on the evolution of Lake Van II: temporal evolution of explosive volcanism of Nemrut Volcano (eastern Anatolia) during the past ca. 0.4 Ma". J. Volcanol. Geotherm. Res. 253, 15–34.
- Sumita, M., Schmincke, H.U., 2013b. "Erratum to Impact of volcanism on the evolution of Lake Van II: temporal evolution of explosive volcanism of Nemrut Volcano (eastern Anatolia) during the past ca. 0.4 Ma". J. Volcanol. Geotherm. Res. 253, 131-33.
- Sumita, M., Schmincke, H.U., 2013c. "Impact of volcanism on the evolution of Lake Van I: evolution of explosive volcanism of Nemrut Volcano (eastern Anatolia) during the past >400,000 years". Bull. Volcanol. 75, 714–715.

- Şaroğlu, F., Yılmaz, Y., 1984. Doğu Anadolu'nun Neo-Tektoniği ve İlgili Magmatizması, Ketin Sempozyumu. Ankara, 149-162.
- Şaroğlu, F., Yılmaz, Y., 1986. Doğu Anadolu'da neotektonik dönemdeki jeolojik evrim ve havza modelleri. MTA Bult., 107: 73-94.
- Uysal İT, Feng Y, Zhao J, Bolhar R, Işık V, Baublys KA, Yago A, Golding SD 2011. "Seismic cycles recorded in late Quaternary calcite veins: geochronological, geochemical and microstructural evidence". Earth Planet Sc Lett 303: 84-96.
- Ünal-İmer, E., Shulmeister, J., Zhao, J.X., Uysal, I.T., Feng, Y.X., Nguyen, A.D. and Yüce, G., 2015. "An 80 kyr-long continuous speleothem record from Dim Cave, SW Turkey with paleoclimatic implications for the Eastern Mediterranean". Scientific reports, 5, 13560.
- Wick, L., Lemcke, G., Sturm, M., 2003. "Evidence for Lateglacial and Holocene climatic change and human impact in eastern Anatolia: high-resolution pollen, charcoal, isotopic and geochemical records from the laminated sediments of Lake Van". Turkey. Holocene. 13, 665-675.
- Yeğen, ŞB., 2021. Tazekent Köyü (Diyadin-Ağrı) Travertenlerinin Jeolojik Özellikleri. (Yüksek Lisans Tezi). Van Yüzüncü Yıl Üniversitesi, Fen Bilimleri Enstitüsü, Van.
- Yeşilova, Ç., Gülyüz, E., Ci-Rong, H., Shen, C-C., Giant tufas of Lake Van record lake-level fluctuations and climatic changes in eastern Anatolia, Turkey. *Palaeogeography, Palaeoclimatology, Palaeoecology*. 533. <https://doi.org/10.1016/j.palaeo.2019.05.048>
- Yeşilova, Ç., Yeğen, ŞB., 2025. Tazekent (Diyadin, Ağrı) Travertenlerinin Oluşum koşulları, ve İlk İklimsel Kanıtları. Türkiye Jeoloji Bülteni, 68(4):1-16. <https://doi.org/10.25288/tjb.1519961>
- Zaman, M., Polat, S., Özdemir, M., 2000. Diyadin thermal springs. Eastern Geographical Review, 4: 349-377.

# CHAPTER 4

## EFFECT OF FACIES PROPERTIES ON PHYSICOMECHANICAL PROPERTIES: HEYBELİ TRAVERTINES (ADİLCEVAZ, BİTLİS)

*Çetin YEŞİLOVA*<sup>1</sup>

*Halit UVAÇIN*<sup>2</sup>

*Hakan ELÇİ*<sup>3</sup>

---

1 Doç. Dr., Yüzüncü Yıl University Department of Geological Engineering, 65080, VAN, TURKEY ORCID ID: 0000-0002-8884-0842, [cetinyesilova@yyu.edu.tr](mailto:cetinyesilova@yyu.edu.tr)

2 Senior Geological Engineer., Yüzüncü Yıl University Institute of Science, 65080, VAN, TURKEY ORCID ID: 0000-0003-2910-7955, [nicavu.65@gmail.com](mailto:nicavu.65@gmail.com)

3 Prof Dr., Dokuz Eylül University Torbalı Vocational Scholl, 35860, İZMİR, TURKEY ORCID ID: 0000-0003-2945-2548, [hakan.elci@deu.edu.tr](mailto:hakan.elci@deu.edu.tr)

## Introduction

The use of stones by humans is almost equivalent to the history of humanity. This journey, which started as a cutter and crusher, has reached inconceivable dimensions today. The most common of these is their use as building stones. Travertines are one of the most sought-after building stones, as they are used both in construction, decoration and even cladding.

Travertine is formed by the precipitation and accumulation of calcium carbonate along fault lines where calcium and bicarbonate-rich groundwater reaches the surface (Pedley, 1990; Ford and Pedley, 1996; Guo and Riding, 1998; Pentecost, 2005; Gandin and Capezuoli, 2008). Due to these properties, travertines are mostly found in geothermal fields following a fracture system (Muir-Wood, 1983; Chafetz and Folk, 1984; Sibson et al., 1975; Altunel and Hancock, 1993b; Guo and Riding, 1998; Fouke et al., 2000; Pentecost, 2005; Veysey et al., 2008; Guido et al., 2010; Guido and Campbell, 2011; Yeşilova et al., 2015a,b, 2017, 2019, 2021; Yeşilova, 2019, 2022). There are many parameters affecting the formation and morphology of travertines, the most important of which are paleomorphology, tectonism, climate and volcanism (Ordonez et al., 1986; Altunel and Hancock, 1993b; Pentecost, 1995; Guo and Riding, 1998; Capezuoli et al., 2009; Brogi and Capezuoli, 2014).

Heybeli Travertines are located in the east of Adilcevaz District (Bitlis), north of Lake Van. These travertines, located right next to the Erciş (Van) - Adilcevaz (Bitlis) highway, surface in an area of approximately 1.5 km<sup>2</sup> (Fig. 1A).

The study aims to compare the effects of facies features on structural features of Heybeli travertines. For this purpose, 56 m. core drilling was carried out from travertines that are almost 80% covered, samples were taken based on these cores and the same structural tests were applied to samples in different facies and changes were monitored according to facies.

## Geology

The study area is located in the Lake Van basin. The basin began to thicken and rise with the compression regime that started 19 ma ago (Gül-yüz et al., 2019). With this compression regime, many large and small faults were formed in the basin. After this fault formation, the drainage system of the existing depression was closed as a result of the eruptions of the Nemrut Volcano approximately 600 ka ago and the Lake Van basin was formed (Degens and Kurtman, 1978). Intense evaporites are observed in the study area and its surroundings as a result of the shallowing and

continentalization that developed due to this uplift (Güngör et al., 2006a, b; Güngör-Yeşilova and Gökmen, 2020; Güngör-Yeşilova et al., 2020; Güngör-Yeşilova and Baran, 2023).

The units in the study area are listed from oldest to youngest as Miocene Adilcevaz limestone, Quaternary Süphan volcanics, Quaternary Van Lake formation and Heybeli travertines and tufas and Quaternary alluviums. Of these units, Miocene Adilcevaz limestones form the bottom layer and are unconformably overlain by Quaternary Süphan volcanics (Uvaçın, 2022). Süphan volcanics are unconformably overlain by Quaternary Van Lake formation and Heybeli travertines and tufas, which are the subject of this study. Quaternary alluvium covers all these units (Figure 1B) (Uvaçın, 2022). Adilcevaz Limestone is observed in the north of the study area, is generally cream-yellow in color, has many fractures and cracks. Süphan Volcanics are observed in the west of the study area. It is black-smoky in color and has basaltic properties. The majority of the cultivated lands in the study area consist of alluvium. In many areas, the alluviums are transitional with the old sediments of Lake Van. These travertines, which are the subject of the study, were formed as a result of the activity of two different faults intersecting each other. These yellow, beige, gray, white and cream colored travertines surfaced between 1670 m and 1725 m in height with a thickness of approximately 55 meters. Onyxes were observed in some levels (Aranlı, 2021; Yeşilova and Aranlı, 2025).

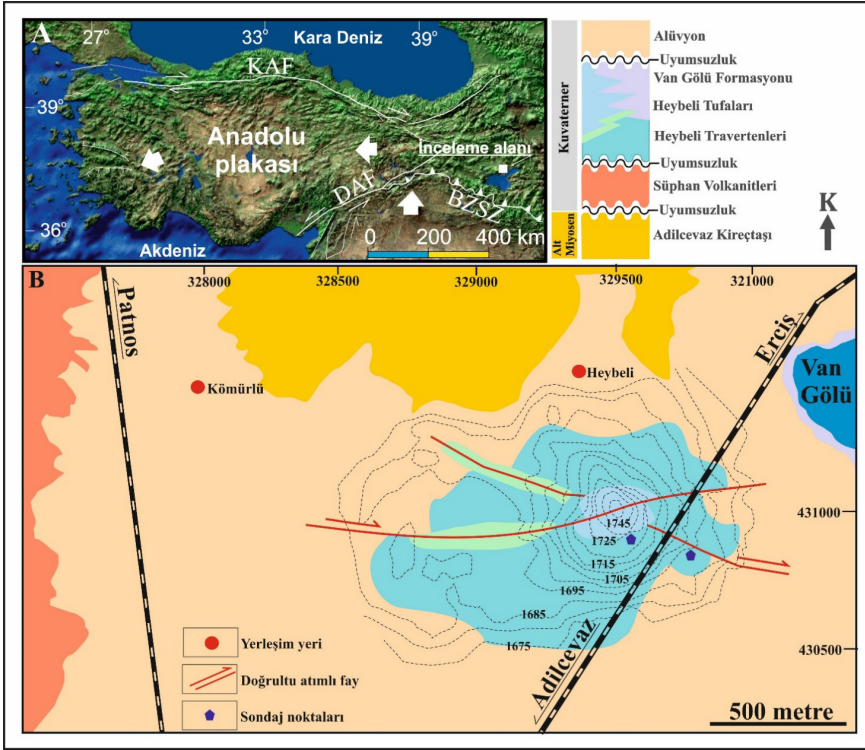


Figure 1. A) Map showing the location of the study area. B) Geological map of the study area (taken from Yeşilova and Aranlı, 2025).

### Heybeli Travertines

Heybeli travertines were classified into facies based on previous studies (Aranlı, 2021; Uvaçin 2022; Yeşilova and Aranlı, 2025). While classifying, lithological features such as composition, texture, layering characteristics and sedimentary structures were taken into account based on the classification made by Guo and Riding (1998). These facies are;

1. Brecciated-lithoclastic facies,
2. Crystalline crust facies
3. Shrub type facies,
4. Paper-thin raft type facies,
5. Coated gas bubble facies, 5 different facies were determined (Aranlı, 2021; Uvaçin 2022; Yeşilova and Aranlı, 2025) (Fig. 2).

***Brecciated-lithoclastic facies***

The facies in question is formed by fragments of different shapes and sizes that are broken off from the existing travertine formation and re-join the travertine formation (Fig. 3 A). However, at the lowest level of the travertines, during the travertine formation, there are also extractclasts (basalt and andesite fragments belonging to Süphan Volcanics) included in the environment along with the travertine fragments. The travertines in question form brecciated extractclast travertines in this form. However, in this study, as in Aranlı, 2021, both facies will be examined under the title of brecciated lithoclast facies. The gray-yellow colored facies repeats 4 times throughout the entire section (Uvaçin, 2022).

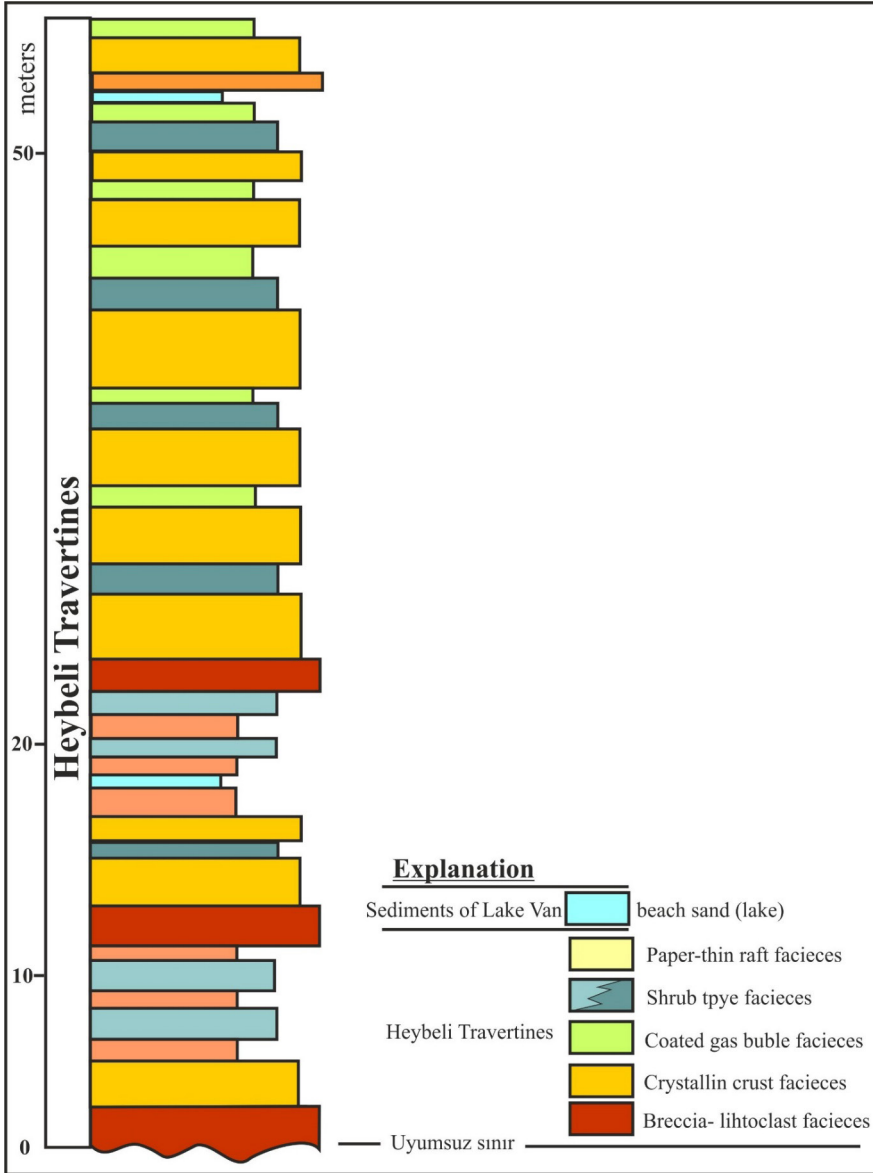


Figure 2. Column section of Heybeli basin facies (taken from (Aranlı, 2021; Uvaçin 2022; Yeşilova and Aranlı, 2025)

### Crystalline crust facies

This facies, which generally represents spring mouths and hot waters (Guo and Riding, 1998), is composed of coarse fibrous and perpendicular calcite crystals to the crystallization surface (Özkul et al., 2002). In the

field, two different onyx formations were observed, cream-beige-yellow or gray. The gray ones are porous and thin-layered (Fig. 3 B).

### *Shrub type facies*

This facies is the most widespread and thick travertine lithofacies of shallow, wide pool and swamp-like environments of low-slope depositional environments and depression areas (Guo and Riding, 1992, 1998; Özkul et al., 2002). Shrubs are formations that expand upwards, develop as dendritic or shrub/dwarf plants (Özkul et al., 2002). It is one of the most repeated facies in the section. It is creamy white in color, thin to medium-layered. It was observed in the field in two different forms as ball-like dwarf shrubs and as sheets (Fig. 3 C).

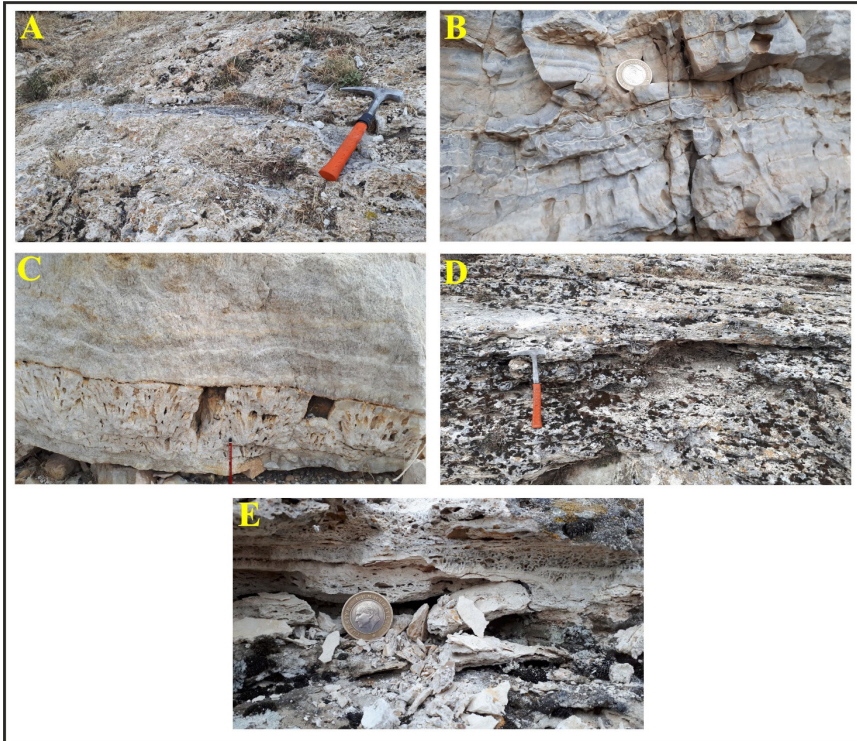


Figure 3. Facies determined in Dereiçi travertines. A) Brecciated-lithoclastic facies, B) Crystalline crust facies, C) Shrub type facies, D) Paper-thin raft facies, E) Coated gas bubble facies.

### ***Paper-thin raft facies***

The travertines forming the raft type facies are formed by the occasional collapse of the CaCO<sub>3</sub> film accumulated on the water surfaces filling the shallow depression areas or terrace pools observed on the travertine formation (Guo and Riding, 1998). This type of travertines are in the form of loose (fragile) thin crystalline layers (Guo and Riding, 1998). It is repeated 5 times along the core taken. Some parts can be observed with the naked eye in the field (Fig. 3 D). The layer thicknesses vary from thick lamina to very thin layers. It is gray-beige in color and represents the lake/pool environment.

### ***Coated gas bubble facies***

This facies, like the raft type facies, is repeated 5 times throughout the section. The facies, which is thin-thick layered, is cream-beige in color (Fig. 3 E). Gas-pocket facies are frequently observed together with crystalline crust, raft and reed type travertine facies. As a result of detailed examinations, gas cavities are frequently observed in other facies (except for the beige-yellow crystalline crust facies). The main reason for this is thought to be the Süphan Volcanism that developed simultaneously with the travertine formation.

## **Method**

The study consists of 3 parts, (i) field studies, (ii) drilling studies (Fig. 4) and (iii) laboratory studies.



Figure 4. Core drilling in Heybeli travertines (A) and a view of the cores obtained (B).

In the field studies, the region was examined in detail, the areas where the travertines were exposed were determined and sampling studies were carried out. In the drilling studies, the travertines were cut from top to ceiling. In this way, the entire stack was obtained with very little loss. Laboratory studies were carried out at Dokuz Eylül University Torbalı Vocational School. Thin sections and physical mechanical tests of the samples were carried out here. Physical experiments were carried out on the samples and experiments were carried out to obtain apparent density, open porosity, true density, total porosity, water absorption value and ultrasonic velocity measurements. In the mechanical tests, compressive strength, point lo-

ading, indirect and direct tensile tests were carried out to determine the strength values of the samples.

### Malzeme Özellikleri

Total Core Yield (TCY%), Intact Core Yield (ICY%) and Rock Quality Indicator (RQI%) values of travertines were calculated from the cores obtained by drilling in Heybeli travertines. In the light of this data, the facies with high values in travertine facies were determined as crystalline crust facies and brecciated-lithoclastic facies. Although the core productivity of other facies was high, the rock quality indicator was very low (Table 1).

Table 1. Determination of discontinuity properties of travertines.

TCY (%)	ICY (%)	RQI (%)	Facies
6,88	5,63	1,25	Shrub type facies
94,66	92,33	65,67	Crystalline crust facies
73	71	0	Coated gas bubble facies
20	8	0	Paper-thin raft facies
62	56	27,5	Brecciated-lithoclastic facies

Physical properties of Heybeli travertine facies were determined by laboratory tests. Among the physical properties, apparent density, open porosity, water absorption values, real density and total porosity were determined separately according to facies.

Table 2. Apparent density, open porosity and water absorption values of travertines.

Facies	Weight in Water (gr) (MH)	Saturated Weight (gr) (MS)	Dry Weight (gr) (MD)	Apparent Density (Kg/m <sup>3</sup> ) (Pb)	Open Porosity (%) (Po)	Water Absorption (%) (Ab)
Brecciated-lithoclastic facies	103.14	166.6	164.93	2.59	2.63	1.01
Brecciated-lithoclastic facies	107	178.34	174.1	2.43	5.94	2.44
Brecciated-lithoclastic facies	110.45	185.32	181.48	2.41	5.13	2.12

Crystalline crust facies	114.38	188.13	182.23	<b>2.46</b>	<b>8.00</b>	<b>3.24</b>
Crystalline crust facies	100.06	166.04	159.61	<b>2.41</b>	<b>9.75</b>	<b>4.03</b>
Crystalline crust facies	107.05	178.73	173.16	<b>2.41</b>	<b>7.77</b>	<b>3.22</b>
Crystalline crust facies	111.09	183.87	180.12	<b>2.46</b>	<b>5.15</b>	<b>2.08</b>
Coated gas bubble facies	87.65	145.93	141.95	<b>2.43</b>	<b>6.83</b>	<b>2.80</b>
Coated gas bubble facies	84.35	143.56	135.33	<b>2.28</b>	<b>13.90</b>	<b>6.08</b>
Coated gas bubble facies	124.51	218.43	205.24	<b>2.18</b>	<b>14.04</b>	<b>6.43</b>
Paper-thin raft facies	102.7	173.06	168.51	<b>2.39</b>	<b>6.47</b>	<b>2.70</b>
Paper-thin raft facies	116.45	271.46	270.16	<b>1.74</b>	<b>0.84</b>	<b>0.48</b>
Shrub type facies	99.1	166.65	158.77	<b>2.34</b>	<b>11.67</b>	<b>4.96</b>
Shrub type facies	103.93	172.8	166.46	<b>2.41</b>	<b>9.21</b>	<b>3.81</b>
Shrub type facies	110.74	185.21	178.4	<b>2.39</b>	<b>9.14</b>	<b>3.82</b>

Compressive strength test was performed on 11 samples taken from Heybeli travertine facies according to TS EN 1926 standards. The purpose of this test is to calculate the performance of travertines in their areas of use (Table 3).

Table 3. Uniaxial compressive strength test data of travertines.

Diameter (mm)	Area (cm <sup>2</sup> )	Load (kgf)	Strength	Facies
44.31	15.41	3690.47	<b>239.45</b>	Brecciated-lithoclastic facies
44.73	15.71	4051.32	<b>257.95</b>	Brecciated-lithoclastic facies
44.94	15.85	3657.67	<b>230.71</b>	Crystalline crust facies
44.8	15.76	7561.36	<b>479.93</b>	Crystalline crust facies
45.13	15.99	11366.65	<b>710.94</b>	Crystalline crust facies
42.31	14.05	1361.37	<b>96.88</b>	Coated gas bubble facies
43.94	15.16	1820.63	<b>120.12</b>	Coated gas bubble facies
45.02	15.91	1525.39	<b>95.87</b>	Paper-thin raft facies
54.5	23.32	1565.58	<b>67.14</b>	Paper-thin raft facies
44.38	15.46	2903.17	<b>187.77</b>	Shrub type facies
42.94	14.47	1951.85	<b>134.85</b>	Shrub type facies

## Discussion and Conclusion

When field observations and facies properties are evaluated, all other travertines except for raft type travertines have an economic value. Shrub type and gas void travertines can be used in decoration, while brecciated and crystalline facies can be used in coating and block production. Especially crystalline shell facies is extremely important because it has onyx properties. However, raft type facies is economically important because it is very fragile.

When the post-examination study carried out on Heybeli travertine mass, the characteristics of the discontinuities determined from the cores taken by drilling and the facies properties are evaluated together, it is seen that only blocks that can be considered economical (1.8-2.6 m<sup>3</sup>) can be produced in travertines belonging to crystalline shell facies. It is not possible to produce economical travertine blocks from other facies. Discontinuities within the travertine mass (low-slope layer planes) limit the volume of blocks that can be obtained to a maximum of 1 m<sup>3</sup>.

The apparent density of Heybeli travertines varies between 2.34 -2.59 g/cm<sup>3</sup>. The facies with the highest apparent density is the crystalline crust facies. The lowest is the gas-porous facies. Since the apparent density is related to the porosity of the travertines, the density of the facies with high porosity is lower.

Heybeli travertines spread over an area of approximately 1.5 km<sup>2</sup> in the region. The thickness of the travertine stack was measured as 54 meters by core drilling. Discontinuities in the travertine stack are generally bedding planes and have a very low slope angle (5-10 degrees). The RQI values of the cores taken from the drilling are greater than 50% only between 16-28 meters. RQI values in the rest of the stack are between 10-25%. The distance between discontinuities in the stack is narrow-closely spaced.

According to the block volumes calculated from RQI values and  $J_v$  values, economic blocks can only be produced from the crystalline crust facies.

As a result of the physical-mechanical tests carried out by taking into account the distinguished facies, the apparent density of the travertine facies is between 2340-2470 kg/m<sup>3</sup> and the open porosity is between 5-10%. With these features, Heybeli travertines are in the class of low-density, highly porous rocks.

In the experiments, it was determined that the lithological properties of the facies include the determining/limiting parameters of the physi-

cal-mechanical properties of the travertines and that the facies properties directly affect the material properties.

Considering the thicknesses, the thickest facies is the crystalline crust facies with 1.5. This facies, which is determined to be 45 meters below the travertine stack, is no longer economical due to the thick travertine stack on it. For this reason, Heybeli Travertines do not have any economic meaning.

### **Acknowledgements**

This study was supported by Yüzüncü Yıl University Scientific Research Project Council (Van YYÜ, BAP, Project No: FLY-2020-8933).

This study was derived from the master's thesis titled "Relationship between Facies Properties of Heybeli (Adilcevaz-Bitlis) Travertines and Material Properties".

## References

- Altunel, E., Hancock, P.L., 1993b. Active fissuring faulting in Quaternary travertines at Pamukkale, western Turkey. *Zeitschrift für Geomorphologie Supplement-Band*, 94: 285-302.
- Aranlı, B., 2021. Heybeli-Kömürlü Köyleri (Adilcevaz, Bitlis) Arasında Yüzeyleyen Travertenlerin Sedimantolojik Özelliklerinin İncelenmesi ve Ekonomik Önemi. Van Yüzüncü Yıl Üniversitesi, Fen Bilimleri Enstitüsü, Van. Yüksek Lisans Tezi (basılmamış).
- Brogi, A., Capezzuoli, E., 2014. Earthquake impact on fissure-ridge type travertine deposition. *Geological Magazine* 151 (6): 1135–1143.
- Capezzuoli, E., Gandin, A., Pedley, M., 2014. Decoding tufa and travertine (fresh water carbonates) in the sedimentary record: The state of the art. *Sedimentology*, 61: 1–21.
- Chafetz, H.S., Folk, R.L., 1984. Travertines: depositional morphology and the bacterially constructed constituents. *Journal of Sedimentary Petrology*, 54: 289–316.
- Degens, E.T., Kurtman, F., 1978. *The Geology of Lake Van*. Maden Tetkik ve Arama Enstitüsü Yayınları, Yay. No: 169, Ankara. 158.
- Ford, T.D., Pedley, H.M., 1996. A review of tufa and travertine deposits of the world. *Earth-Science Reviews*, 41: 117–175
- calcite in hot-spring travertines, central Italy. *SEPM Special Publication*, 36: 349-369.
- Ford, T.D., Pedley, H.M., 1996. A review of tufa and travertine deposits of the world. *Earth-Science Reviews*, 41: 117–175.
- Fouke, B.W., Farmer, J.D., Des Marais, D.J., Pratt, L., Sturchio, N.C., Burns, P.C. and Discipulo, M.K., 2000. Depositional facies and aqueous-solid geochemistry of travertine-depositing hot springs (Angel Terrace, Mammoth Hot Springs, Yellowstone National Park, U.S.A.). *Journal of Sedimentary Research*, 70: 565–585.
- Gandin, A., Capezzuoli, E., 2014. Travertine: distinctive depositional fabrics of carbonates from thermal spring systems. *Sedimentology* 61: 264–290
- Guo, L., Riding, R., 1998. Hot-spring travertine facies and sequences, Late Pleistocene Rapolano Terme, Italy. *Sedimentology*, 45: 163–180.
- Guo, L. and Riding, R., 1992. Aragonite laminae in hot water travertine crust, Rapolano Terme, Italy. *Sedimentology*, 39: 1067–1079
- Guido, D.M., Channing, A., Campbell, K.A., Zamuner, A., 2010. Jurassic geothermal landscapes and fossil ecosystems at San Agustín, Patagonia, Argentina. *Journal of Geological Society, London*, 167: 11–20.
- Muir-Wood, R., 1993. Neohydrotectonics. *Z. Geomorphology Supplementary*, 94: 275–284.

- Guido, D.M., Campbell, K.A., 2011. Jurassic hot spring deposits of the Deseado Massif (Patagonia, Argentina): characteristics and controls on regional distribution. *Journal of Volcanology and Geothermal Research*, 203: 35–47.
- Gülyüz, E., Durak, H., Özkaptan, M., Krijgsman, W., 2019. Paleomagnetic constraints on the early Miocene closure of the southern Neo-Tethys (Van region; East Anatolia): Inferences for the timing of Eurasia-Arabia collision. *Global and Planetary Change*, 185, 103089. <https://doi.org/10.1016/j.gloplacha.2019.103089>
- Güngör, P., Yeşilova, Ç., Çiftçi, Y., 2006a. **Van Gölü KB-GD Kesimlerinin Senozoyik Stratigrafisi**. 30. Yıl Fikret Kurtman Jeoloji Sempozyumu, Konya, Türkiye, 20 - 23 Eylül 2006, ss.223-224
- Güngör, P., Yeşilova, Ç., Çiftçi, Y., 2006b. **Timar Bölgesindeki (Van Gölü Doğusu) Jipslerin Oluşumuna Ön Yaklaşım**. 59. Türkiye Jeoloji Kurultayı, Ankara, Türkiye, 20 - 24 Mart 2006, ss.215-216.
- Güngör Yeşilova, P., Gökmen, D., 2020. The paleodepositional environment, diagenetic and depositional conditions of the Middle-Late Miocene Koluz gypsum member (NE Van, Eastern Turkey). *Carbonates and Evaporites*, 35: 2–21.
- Güngör Yeşilova, P., Yeşilova, Ç., Açlan, M., Gundogan, I., 2020. Geochemical characteristics of gypsum lithofacies in northeastern of Mus (Eastern Anatolia-Turkey): an indication of the Neotethys closure. *Carbonates and Evaporites*, 35: 1-18.
- Güngör Yeşilova, P., Baran, O., 2023. **Origin and Paleoenvironmental Conditions of the Köprübaşı Evaporites (Eastern Anatolia, Turkey): Sedimentological, Mineralogical and Geochemical Constraints**. *Minerals* , 13(2): 1-21
- Ordenez, S., Gonzalez, J.A., Garcia del Cura, M.A., 1986. Petrographie et morphologie desidifices tuffeux quaternaires du centre de l'Espagne, *Mediterranean*, 1–2: 52–60.
- Özkul, M., Varol, B., Alçiçek, M.C., 2002. Depositional environments and petrography of the Denizli travertines. *Bulletin of Mineral Research Exploring*, 125: 13–29.
- Pedley, H.M., 1990. Classification and environmental models of cool freshwater tufas. *Sedimentary Geology*, 68: 143–154.
- Pentecost, A., 1995. The Quaternary travertine deposits of Europe and Asia Minor. *Quaternary Science Reviews*, 14: 1005–1028.
- Pentecost, A., 2005. *Travertine*. Springer, Berlin, 446 pp.
- Sibson, R.H., Moore, J.M.M., Rankin, A.H., 1975. Seismic pumping a hydrothermal fluid transport mechanism. *Journal of the Geological Society*, 131: 653–659.

- Uvaçın, H., 2022. Heybeli (Adilcevaz-Bitlis) Travertenlerinin Fasiyes Özelliklerinin Malzeme Özellikleriyle İlişkisi. Van Yüzüncü Yıl Üniversitesi, Fen Bilimleri Enstitüsü, Van. Yüksek Lisans Tezi (basılmamış).
- Veysey, J., Fouke, B.W., Kandianis, M.T., Schickel, T.J., Johnson, R.W. and Goldenfeld, N., 2008. Reconstruction of water temperature, ph, and flux of ancient hot springs from travertine depositional facies. *Journal of Sedimentary Research*, 78: 69-76.
- Yeşilova, Ç., 2019. Preliminary approach to paleogeographic properties of Edremit (Van) Travertines, eastern Turkey. IESCA, 60p. 7-11 October 2019, İzmir.
- Yeşilova, Ç., Güngör Yeşilova, P., Açlan, M.,** 2015a. Edremit (Van) Travertenlerinin Fasiyes Analizi (in Turkish). 68. Türkiye Jeoloji Kurultayı, 578-579, Ankara, Türkiye
- Yeşilova, Ç., Üner, S., Güngör Yeşilova, P., Açlan, M., Alırız, M.G. 2015b. Kuvarterner Yaşlı Edremit Travertenleri'nin Fasiyes Özellikleri ve Oluşum Ortamları (Van Gölü Havzası-Doğu Anadolu) (in Turkish). Traverten - Tufa Çalıştayı, Pamukkale Üniversitesi Mühendislik Fakültesi, Denizli. 54-55.
- Yeşilova, Ç., Açlan, M., Güngör Yeşilova, P., (2017). Dereiçi Travertenlerinin Sedimantolojik Özellikleri ve Jeomiras Ögelerinin Değerlendirilmesi. Sedimantoloji Çalışma Grubu\_2017 (pp.28-29). Rize Türkiye
- Yeşilova, Ç., Gülyüz, E., Huang, C.-R., Shen, C.-C. (2019). Giant tufas of Lake Van record lake-level fluctuations and climatic changes in eastern Anatolia, Turkey. *Palaeogeography, Palaeoclimatology, Palaeoecology*, 533, 109226.
- Yeşilova, Ç., Güngör-Yeşilova, P., Açlan, M., Tsai-Luen, Y., Chuan-Chou, S., 2021. U-Th ages and Facies Properties of Edremit Travertine/Tufas, Van, Eastern Anatolia: Implications of Neo-tectonic for the region. *Geological Quarterly* 65(2): 1 – 20.
- Yeşilova, Ç., 2022. Climate and Tectonic Effects on the Origin and Evolution of the Dereiçi Travertines: The Başkale Basin (Eastern Turkey) and Neo-tectonic Implications. *Geological Quarterly* 66(3):, 1 – 20
- Yeşilova, Ç., Aranlı, B., 2025. Gölsel Seviye Değişimleri ve Volkanizmanın, Eşzamanlı Oluşan Traverten ve Tufalar Üzerine etkileri; Heybeli Traverten ve Tufaları (Adilcevaz, Bitlis). *Türkiye Jeoloji Bülteni*. 68(4):77-96